sustainability

MDPI

Article

Anaerobic Co-Digestion of Food Waste in Ghana: Biological Methane Potential and Process Stabilisation Challenges in a Rural Setting

Raquel Arnal-Sierra [1], Simone Colantoni [1], Albert Awopone [2], Isaac Boateng [3], Kingsley Agyapong [4], Frederick Kwaku Sarfo [5], Daniele Molognoni [1,*] and Eduard Borràs [1]

[1] Leitat Technological Center, Department of Circular Economy and Decarbonization, C/de la Innovació 2, 08225 Terrassa, Spain; rarnal@leitat.org (R.A.-S.); eborras@leitat.org (E.B.)
[2] Department of Electrical and Electronics Technology Education, Akenten Appiah-Menka University of Skills Training and Entrepreneurial Development (AAMUSTED), Kumasi P.O. Box 1277, Ghana; aawopone@aamusted.edu.gh
[3] Department of Construction Technology and Management Education, Akenten Appiah-Menka University of Skills Training and Entrepreneurial Development (AAMUSTED), Kumasi P.O. Box 1277, Ghana; isaac.boateng@uew.edu.gh
[4] Department of Management Education, Akenten Appiah-Menka University of Skills Training and Entrepreneurial Development (AAMUSTED), Kumasi P.O. Box 1277, Ghana; kingsleyagyapong@aamusted.edu.gh
[5] Department of Educational Leadership, Akenten Appiah-Menka University of Skills Training and Entrepreneurial Development (AAMUSTED), Kumasi P.O. Box 1277, Ghana; fksarfo@aamusted.edu.gh
* Correspondence: dmolognoni@leitat.org

Abstract

In rural Ghana, limited access to affordable, clean cooking fuels drives the need for decentralised waste-to-energy solutions. Anaerobic co-digestion (AcoD) offers a viable route for transforming organic residues into renewable energy, with the added benefit of improved process stability resulting from substrate synergy. This study aims to evaluate the technical feasibility and stabilisation challenges of AcoD, using locally available fruit waste and beet molasses at a secondary school in Bedabour (Ghana). Biological methane potential (BMP) assays of different co-digestion mixtures were conducted at two inoculum-to-substrate (I/S) ratios (2 and 4), identifying the highest yield (441.54 ± 45.98 NmL CH_4/g VS) for a mixture of 75% fruit waste and 25% molasses at an I/S ratio of 4. Later, this mixture was tested in a 6 L semi-continuous AcoD reactor. Due to the high biodegradability of the substrates, volatile fatty acid (VFA) accumulation led to acidification and process instability. Three low-cost mitigation strategies were evaluated: (i) carbonate addition using eggshell-derived sources, (ii) biochar supplementation to enhance buffering capacity, and (iii) the integration of a bioelectrochemical system (BES) into the AcoD recirculation loop. The BES was intended to support VFA removal and enhance methane recovery. Although they temporarily improved the biogas production, none of the strategies ensured long-term pH stability of the AcoD process. The results underscore the synergistic potential of AcoD to enhance methane yields but also reveal critical stability limitations under high-organic-loading conditions in low-buffering rural contexts. Future implementation studies should integrate substrates with higher alkalinity or adjusted organic loading rates to ensure sustained performance. These findings provide field-adapted insights for scaling-up AcoD as a viable renewable energy solution in resource-constrained settings.

Academic Editor: Francesco Ferella

Received: 28 July 2025
Revised: 19 August 2025
Accepted: 20 August 2025
Published: 22 August 2025

Citation: Arnal-Sierra, R.; Colantoni, S.; Awopone, A.; Boateng, I.; Agyapong, K.; Sarfo, F.K.; Molognoni, D.; Borràs, E. Anaerobic Co-Digestion of Food Waste in Ghana: Biological Methane Potential and Process Stabilisation Challenges in a Rural Setting. *Sustainability* **2025**, *17*, 7590. https://doi.org/10.3390/su17177590

Keywords: anaerobic co-digestion; food residues; biological methane potential; waste management; rural energy access

1. Introduction

Fuel supply for cooking and heating represents a significant challenge in Ghana. Most of the energy for cooking comes from firewood, charcoal and liquefied petroleum gas (LPG), with firewood and LPG being the primary sources. However, this reliance leads to deforestation, health issues from indoor air pollution, and high carbon dioxide emissions [1,2], while rising fuel prices add financial strain on households, schools, and public facilities. There is an urgent need for cleaner, more sustainable, and affordable energy alternatives [3].

Anaerobic digestion (AD) is a promising solution, as it allows the conversion of organic waste into biogas and digestate. Biogas, primarily composed of methane (CH_4) and carbon dioxide (CO_2) [4], can be used as a fuel for cooking, heating, and electricity generation, [5] while digestate serves as a biofertiliser rich in macronutrients [6]. The AD process occurs in four main stages: first, the hydrolysis phase, where complex organic matter is broken down into simpler molecules; second, the acidogenesis phase, where fermentative bacteria convert sugars, amino acids, and long-chain fatty acids into volatile fatty acids (VFAs); third, the acetogenesis phase, where acetogenic bacteria transform the VFAs into acetic acid, hydrogen (H_2), and CO_2; and finally, the methanogenesis, in which methanogenic archaea convert the acetic acid and H_2 into CH_4 [7,8]. Anaerobic digesters are technologically simple and affordable, and can be installed using pre-existing infrastructure such as septic tanks, with minor modifications [9].

The stability and efficiency of AD depend strongly on the characteristics of the substrates used. In particular, fruit and sugary residues are prone to acidification, due to their high biodegradability and rapid accumulation of VFAs. This acidification can inhibit methanogenesis and destabilise the process [10,11]. One widely used approach to mitigate this issue is co-digestion, which involves combining two or more substrates to improve nutrient balance, buffer capacity, and overall stability of the process. Co-digestion has been shown to enhance CH_4 yields and process robustness [12].

The biological CH_4 potential (BMP) test is a standardised method used to determine the CH_4 production capacity of individual or mixed substrates, under controlled anaerobic conditions. The cumulative CH_4 production is measured and normalised based on the volatile solids (VS) content of solid substrates, or the chemical oxygen demand (COD) of liquid substrates [13]. The BMP assay is a useful tool to characterise potential substrates for anaerobic co-digestion (AcoD) and optimise its operational parameters. It has been extensively used to test residues such as wastewaters [14–17], animal manure [18–20], and agro-food residues [8,21,22], among others.

Although many studies have explored BMP and co-digestion in controlled settings, only a few have addressed these approaches under real-world conditions in rural sub-Saharan Africa. In most cases, the information is theoretical [23,24] or relies on chemicals and amendments that would not be possible to implement in the field [25]. The present study aims to address this gap by evaluating AcoD strategies using real, locally available substrates in a specific case study: a secondary school in Bedabour in the Atwima Mponua District of Ghana's Ashanti Region. The school currently consumes approximately two truckloads of firewood and 200 L of LPG per week for cooking. During the implementation of the European project SESA (Smart Energy Solutions for Africa), consultations with school staff and the surrounding community identified two organic waste streams that are regularly and freely available to the school: (i) fruit and vegetable residues from the

nearby Nkawie market and (ii) molasses, a sugar-rich byproduct from a local sugar refinery that the school receives through an informal supply agreement. Although large volumes of organic waste are generated across sub-Saharan Africa, their valorisation through AcoD remains limited due to financial, technical, and infrastructural constraints. In this case, the school plans to retrofit an existing septic tank to function as a digester. This solution prioritises economic viability and ease of implementation, using existing infrastructure to overcome major barriers to AcoD deployment in rural regions.

This study aims to address the critical need for context-specific AcoD strategies in low-resource rural settings by focusing on the real-life case study of a secondary school. To assess the feasibility of biogas production, the BMP of each substrate and their co-digestion mixture (25% molasses and 75% fruits *v*/*v*) was evaluated. Additionally, to address the issue of acidification during the AcoD of these substrates, a second phase of the study involved operating a 6 L anaerobic digester to test three low-cost, locally implementable strategies. The proposed strategies were (i) enhancing initial alkalinity through the addition of carbonate, which could be achieved using eggshells; (ii) the incorporation of biochar, provided by another partner in the SESA project operating in the region; and (iii) removing the excess VFAs through the integration of a bioelectrochemical system (BES) into the AD recirculation loop. BES systems are characterised by the electrical stimulation of electro-active microorganisms, are capable of exchanging electrons with solid elements such as electrodes, and have been extensively applied for waste treatment and the optimisation of conventional AD processes [26,27].

The main gap this study seeks to address is the lack of applied, field-adapted co-digestion strategies that are feasible in resource-limited settings and grounded in real substrate availability. While numerous laboratory-scale studies exist, few have tested stabilisation techniques under the socio-economic and infrastructural constraints typical of rural African communities. This work contributes with practical, scalable, and evidence-based solutions that can support the sustainable deployment of AcoD technology in similar contexts, advancing both waste valorisation and access to renewable energy in developing regions.

2. Materials and Methods

2.1. Substrate and Inoculum

Two different substrates were selected based on the availability of residues in Ghana: molasses from sugar beet and a fruit mixture. The molasses was sourced from the Toro sugar factory in Zamora, Spain, and, due to its high density, was diluted 1:1 with distilled water. Given that beet molasses is a relatively homogeneous byproduct regardless of their production site, the selection of a local supplier in Spain was based on logistical convenience, ensuring consistent quality while minimising transportation constraints [28]. The fruit mixture was selected to reflect the typical types of fruit residues generated by the Nkawie fruit market. To ensure consistency and replicability across experiments, a defined mixture was prepared using equal volumetric parts of plum (1/3), melon (1/3), and watermelon (1/3), chopped and blended until smooth, then used in both the BMP assays and the CSTR reactor. The inoculum used in the BMP assays was anaerobic sludge obtained from the anaerobic digester of the wastewater treatment plant in Terrassa, Spain. All materials were stored in a cold chamber at 4 °C. In the case of the inoculum, only sludge stored for less than two weeks was used to ensure a viable and active microbial community.

2.2. BMP Assays

An Automatic Methane Potential Test System (AMPTS II, BPC Instruments, Lund , Sweden) was used for BMP tests, consisting of 15 sealed reactors, each equipped with a CO_2 absorption unit with NaOH solution and a gas volume measurement unit for standardised CH_4 flow recording [29] (Supplementary Material, Figure S1).

All experiments were carried out in triplicate with 350 mL of working volume, filled with the mixture of inoculum and substrate, and flushed with N_2 for 10 min to ensure anaerobic conditions. They were incubated at 37 °C, and the experiments ended once gas flow was lower than 5 mL per bottle per day. The assays lasted between 15 and 20 days. Three negative controls (just inoculum) and three positive controls (inoculum and cellulose microcrystalline) were performed to assess the endogenous CH_4 production and the inoculum activity, respectively.

Two different I/S ratios were tested for both substrates, calculated based on VS concentration. The first tested ratio was 2, which is commonly recommended for initial substrate evaluations [30]. Given the high concentration of VFAs and the biodegradability of the substrates, a second test was conducted with a ratio of 4, which is more suitable for acidic substrates or those with high sugar and carbohydrate content [7,30–32]. Finally, based on the individual BMP results, a co-digestion experiment was conducted using a substrate mixture of 25% molasses and 75% fruit (*v*/*v*), diluted 1:1 with water, at an I/S ratio of 4. Due to the risk of acidification, the test at an I/S ratio of 2 was not performed in this case. Samples were taken before and after the BMP assays and analysed for pH, conductivity, VFA/Alkalinity, alkalinity, VFAs, COD, ammonium, TN, VS, and TS. The removal of VS and COD were calculated as the difference between the initial and final concentration, divided by the initial concentration, and expressed as a percentage. The experimental scheme of the different combinations is shown in Table 1.

Table 1. BMP assays performed for the three substrates, with two different I/S ratios. Experiments were performed in triplicate. The inoculum was the same for I/S 2 and 4, so the control (+) was not repeated for the I/S 4 trials.

	I/S 2	**I/S 4**
Control (−)	C(−)	C(−)
Control (+)	C(+)	-
Molasses	M2	M4
Fruits	F2	F4
Molasses/Fruits (25:75)	-	MF4

The data from the gas recorder were collected at the end of the experiment and used to calculate the BMP (L CH_4/g VS) according to Equation (1), where V_S (L) is the accumulated volume of CH_4 in the reactor, V_B (L) is the average volume of CH_4 produced by the control (−), m_{IS} (g or mg) is the total amount of inoculum in the sample, m_{IB} (g or mg) is the total amount of inoculum in the control (−), and $m_{vs,ss}$ (g) is the amount of VS from the substrate contained in the reactor [33].

$$BMP = \frac{V_S - V_B \frac{m_{\mathrm{IS}}}{m_{\mathrm{IB}}}}{m_{\mathrm{vs,ss}}} \quad (1)$$

Moreover, the experimental results were compared with the Gompertz model, a widely used model to assess AD [34]. In Equation (2), $G_{(t)}$ is the cumulative CH_4 production at digestion time t (mLCH_4/g VS), G_0 is the BMP of the substrate (mLCH_4/g VS), R_{max} is the maximum CH_4 production rate (mLCH_4/g VS/d), λ is the lag phase (days), t is the

digestion time (days), and *e* is the Euler's number of approximately 2.71828. Excel's Solver Tool was used for the determination of the kinetic constants, and all graphs were plotted in Excel. The model accuracy was assessed by the coefficient of determination R^2 and the mean squared error (MSE) [35].

$$G_{(t)} = G_0 * \exp(-\exp(\frac{R_{\max} * e}{G_0}(\lambda - t) + 1)) \quad (2)$$

2.3. AD Process Optimisation at Lab Scale

After testing and analysing the substrates for biogas production, the optimal co-digestion strategy was applied to operate a scaled-up continuously stirred tank reactor (CSTR). The AD reactor was a jacketed glass unit, with a total volume of 8 L and a working volume of 6 L (Scharlab S.L., Barcelona, Spain) with constant mixing provided through digestate recirculation (150 mL/min). The reactor lid included connections for slurry recirculation (inlet and outlet), a temperature probe (AMR, model FNA30L0250T, Safer Instrumentación S.L., Bilbao, Spain), and a gas outflow line connected with a flow meter (BlueVCount flow meter, BlueSens, Herten, Germany). The flow meter measured the daily biogas production, which was then stored into an external gas bag for weekly compositional analyses (O_2, N_2, CH_4, CO_2, H_2S, H_2). The AD reactor jacket was connected with a thermostatic bath, maintaining a constant internal temperature of 35 °C. Additionally, a pH probe (pH AMR, model FY96PHER, Safer Instrumentación S.L., Bilbao, Spain) was installed in the digestate recirculation line for monitoring and manual adjusting purposes (Figure 1).

The reactor operated for 18 weeks with a hydraulic retention time (HRT) of 30 days. No pH control was applied during the operation. It was inoculated with 4.8 L of anaerobic sludge and collected at the local wastewater treatment plant, and 1.2 L of the optimal substrate mixture was identified during the BMP tests. The mixture (S0) consisted of 75% fruit waste (equal volumetric parts of plum, melon, and watermelon, chopped and blended all together) and 25% molasses, diluted 1:1 with water. The mixture was sieved through a 2 × 2 mm mesh to prevent clogging of the hydraulic circuit.

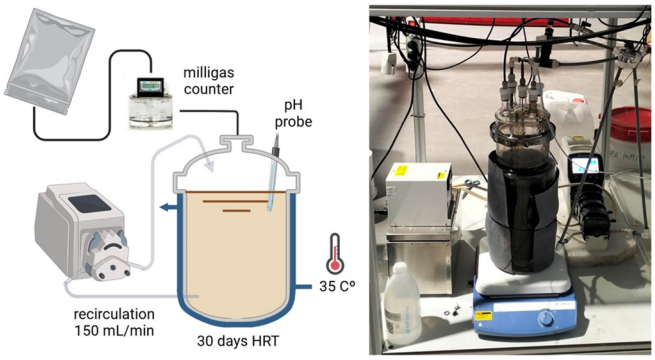

Figure 1. Left, the scheme of the CSTR set-up. Right, a photo of the CSTR in the laboratory.

During the initial 4 weeks, the reactor was fed with the S0 mixture, and periodic adjustments with 1 M NaOH were performed to stabilise pH and support methanogen growth (6.5–8). However, the reactor failed to stabilise and to produce biogas due to acid regression. Three low-cost strategies were tested to address this challenge, suitable for implementation at rural demonstration sites: (S1) increasing initial alkalinity using Na_2CO_3; (S2) adding biochar produced by a project partner; and (S3) incorporating a BES into the AD recirculation loop to consume the excess of VFAs and neutralise the pH. The total experiment was therefore divided into four operational periods: S0 (weeks 1–4), S1 (5–10), S2 (11–14), and S3 (15–18). The operational schedule is shown in Table 2.

Table 2. The operational schedule of the scaled-up AD reactor.

	S0	S1	S2	S3
Week	1–4	5–10	11–14	15–18

During the period S1, the feed mixture was amended with 10 g/L of Na_2CO_3, substituting the $CaCO_3$ found in eggshells, a resource potentially available at the demonstration site in Ghana. The addition of eggshell-derived $CaCO_3$ was shown in previous studies to stabilise pH and mitigate VFA accumulation during AD, improving CH_4 yield and system resilience under acidic stress [36,37]. During the period S2, biochar was incorporated into the feed mixture, which was already amended with 10 g/L of Na_2CO_3. The biochar, produced from wood at 750 °C with particle sizes between 0 and 15 mm (Carbon Cycle, Rieden, Germany; characterisation available in Table S1), was also added at a concentration of 10 g/L [38]. Biochar enhances AD by supporting microbial growth, biofilm formation, and trophic interactions. Additionally, it acts as an adsorbent for inhibitory compounds such as ammonium, hydrogen sulphide, and VFAs, helping to reduce their toxic effects. Its porous structure and conductive properties were also reported to improve electron transfer mechanisms, thereby promoting syntrophic relationships and overall system stability [39]. Between the S1 and S2 trials, a three-week period without feeding allowed the reactor to stabilise and support methanogen population growth.

As a strategy to prevent acid regression, a BES reactor was connected to the recirculation loop (S3). Two rectangular single-chamber BES cells, each with a 0.5 L volume, were constructed from methacrylate and configured with anodes and cathodes submerged in the same electrolyte. Each cell contained four carbon fibre brush anodes and four cathodes, providing a projected surface area of 44.47 cm^2 (Tecnocepillo Befur S.L., Premia del Mar, Spain). The electrodes were connected with stainless steel current collectors, and an Ag/AgCl reference electrode (+0.195 V vs. SHE, Xi'an Yima Opto-electrical Technology, Xi'an, China) was positioned between the rows of anodes and cathodes. The cells were operated in parallel using a power supply (TENMA 72–2715, Farnell, Barcelona, Spain) to control the applied voltage. A multichannel data acquisition system (PicoLog 1216, Farnell, Barcelona, Spain) allowed for monitoring of the cells' performance. Current production was calculated via Ohm's law by measuring the voltage drop across a 1 Ω resistor.

Prior to integration into the recirculation loop, the BES cells were inoculated separately over one week. The inoculation medium consisted of 50% acetate solution and 50% effluent from another BES available in the laboratory as source of electroactive bacteria. The cells were operated at a constant voltage of 0.3 V with an HRT of 15 days. During inoculation, an acetate-based medium [40] was used for the first four days, followed by the S0 mix for the next three days. To protect the electroactive biofilm from the acidic conditions of the main reactor, the reactor pH was adjusted to 7.2 using NaOH prior to BES integration. During BES operation, three different applied voltages (0.3 V, 0.4 V, and 1 V) were tested. The initial voltage of 0.3 V was selected because low voltages are known to favour the development of electroactive biofilms [41]. The subsequent increases to 0.4 V and 1 V were intended to accelerate the consumption of accumulated VFAs.

Digestate (outlet) samples were collected twice per week, and total and volatile solids were measured weekly. On the other hand, inlet samples were collected weekly and subjected to the same analyses. Additionally, the biogas composition was analysed weekly from the gas accumulation bag, while daily biogas production was recorded using the flowmeter at the gas outlet.

2.4. Biogas Yield Estimation from Fruit and Molasses Co-Digestion and Cost Analysis

The theoretical estimation of biogas potential for Nkawie SHS was derived from the experimental BMP obtained in the laboratory co-digestion assays. The CH_4 yield from the optimal mixture (75% fruits, 25% molasses) was recorded as 441.54 ± 45.98 mL CH_4/g VS. This value was used in a mass balance framework to estimate the total biogas production using Equation (3).

$$Biogas\ Yield\ (Nm^3/week) = \frac{VS(kg/week) \times BMP(mL\ CH_4/g\ VS)}{1000} \quad (3)$$

The total volatile solid content in the weekly waste stream (2000 kg fruit and 500 kg molasses) was computed using the laboratory-measured values VS concentrations (fruit ≈ 92.9 g/kg and molasses ≈ 283.96 g/kg). The calculated CH_4 output was then converted into energy using the lower heating value (LHV) of CH_4, assumed to be 35.8 MJ/Nm^3 under standard conditions, assuming 100% conversion efficiency and no energy losses. This approach, grounded in experimental data, ensures an evidence-based projection of the biogas potential and energy yield for the school setting. Additional details and calculations are provided in the Supplementary Material.

The theoretical estimation method aligns with the AMPTS-II standard BMP calculation protocol, and the kinetic validation via the Gompertz model ensures its reliability. Similar yield extrapolation methods were used in substrate feasibility studies [42,43].

The economic viability of implementing biogas technology at Nkawie SHS was evaluated using a simplified life-cycle cost analysis (LCCA). The analysis comprised the following:

- Capital Expenditure (CAPEX): Based on regional estimates for constructing fixed-dome digesters in Ghana, ranging between USD 10000 and USD 50000.
- Operational Expenditure (OPEX): Annual maintenance costs were estimated at USD 500/year.
- Fuel Savings: The current weekly consumption of two truckloads of wood and 200 L of LPG was costed using prevailing market prices in Ghana to determine annual savings.
- Refuse Disposal Costs: The school currently spends approximately USD 1500 annually on waste disposal, which could be reduced with on-site digestion.
- Payback Period: Estimated by dividing the total investment by the annual cost savings derived from reduced fuel and waste disposal expenses.

The cost analysis followed the simplified LCCA guidelines as applied in institutional contexts by the Africa Biogas Partnership Program [5] and further detailed in ref. [44], which evaluates both direct savings and environmental co-benefits.

2.5. Analysis and Characterisation

The same set of analyses was performed for the substrates, inocula, and digestate samples of the BMP assays as well as throughout the monitoring of the AD reactor. The analyses included the determination of the chemical oxygen demand (COD) (Kit LCK 014, method LCK 514, Hach, Düsseldorf, Germany), pH and conductivity (Hach Lange HQ44OD, Hach, Düsseldorf, Germany), alkalinity and VFA/Alkalinity (TitraLab AT1000, Hach, Düsseldorf, Germany), total nitrogen (TN) (Kit LCK method 338, Hach, Düsseldorf, Germany), and ammonia nitrogen (Kit LCK 303, method 503, Hach, Düsseldorf, Germany). The C/N ratio was calculated as COD/TN. The VFA concentration was calculated as the product between the alkalinity and the VFA/Alkalinity ratio. The total solids (TS) and volatile solids (VS) were determined by heating each sample in the muffle up to 105 °C for 8 h and then up to 550 °C for 4 h, respectively (Stove MEMMERT UF55, Memmert GmbH + Co. KG, Schwabach, Germany). Finally, an estimation of the calorific value of the

biogas produced was calculated using the standard value of 35.8 MJ/m^3 for pure CH_4 by multiplying this factor by the average CH_4 concentration (%) obtained in each experimental condition.

3. Results and Discussion

3.1. Substrate Characterisation

The composition and the key parameters for the BMP of the two substrates and the inoculum were analysed. The results of the characterisation are shown in Table 3, along with the optimal values per parameter. The measurements were performed in triplicates.

Table 3. Characterisation results and optimal range of parameters for BMP experiments.

	Molasses	Fruit Mix	Inoculum	Optimal Range [30]
pH	7.19 ± 0.06	4.23 ± 0.57	7.2 ± 0.01	6.5–8
Conductivity (mS/cm)	20.41 ± 0.01	4.52 ± 0.22	6.7 ± 0.2	-
NH_4-N (mg/L)	24.60 ± 1.69	62.5 ± 7.7	1165 ± 0.02	<2500
COD (g/L)	341.65 ± 12.69	123.9 ± 2.9	49.7 ± 0.42	-
Total nitrogen (g/L)	0.69 ± 0.02	1.2 ± 0.77	3.54 ± 0.08	-
C/N	495 ± 38	131 ± 87	14 ± 0.21	10–90
VFA/Alkalinity	4.50 ± 0.04	2.42 ± 0.01	0.5 ± 0.02	0.3–0.4
Alkalinity (g $CaCO_3$/L)	16.20 ± 0.17	2.91 ± 0.05	2.7 ± 0.05	>3 [45]
VFA (g/L)	73.5 ± 1.45	7.71 ± 0.95	1.4 ± 0.08	<1
Total solids TS (g/L)	340.26 ± 2.48	99.83 ± 1.19	46.6 ± 0.57	-
Volatile solids VS (g/L)	283.96 ± 4.91	92.90 ± 11.9	32.4 ± 0.18	20–60

The selected substrates presented various challenges for BMP. The VFA/Alkalinity was notably high (4.50 ± 0.04 for molasses and 2.40 ± 0.01 for fruit mix), whereas its ideal value should be between 0.3 and 0.4 [13]. Both substrates exhibited high concentrations of VFAs and relatively low alkalinities. Molasses, a byproduct of sugar processing, primarily consists of simple sugars, making it highly degradable [46]. During the acidogenesis stage, molasses degradation can cause a significant drop in pH, leading to process inhibition due to organic overload [47]. Similarly, the fruit mix, also rich in VFAs and possessing an acidic pH, could lead to rapid pH-related inhibition [48]. The optimal pH for AD is between 6.5 and 8 [49], so the low pH of the fruit mix posed potential challenges to the AD process.

The C/N ratio of both substrates was higher than optimal, as they contained substantial organic matter but were low in protein. However, since the used inoculum had a relatively low C/N ratio and a higher proportion of inoculum was employed, the final C/N ratio of the co-digestion fell within the optimal range. Ammonium concentration, which can inhibit methanogenesis at levels above 2500 mg/L [50], was low in the experiments. Conductivity, an indirect indicator of salt content, is critical, as high salt concentrations can be toxic to microorganisms. Prior studies indicate moderate inhibition at salt levels between 3.5 and 55 g/L [51]. Molasses initially had the highest conductivity, but dilution with inoculum reduced it from 20.41 mS/cm to 8.17 (I/S = 2) and 12.9 mS/cm (I/S = 4). These values were consistent with those reported in other BMP studies involving molasses and fruits.

3.2. BMP Results

3.2.1. Individual BMP

I/S Ratio of 2

The average BMP recorded for molasses (test M2) was 292 ± 9.04 NmL CH_4/g VS, in agreement with the literature. In previous studies, BMP values for sugar beet molasses typically ranged from 250 to 500 NmL CH_4/g VS, with the lower values often linked to acidification or salinity effects and the higher yields achieved under optimised or co-digestion conditions [42,43]. On the other hand, the average BMP for the fruit mix (test F2) was 175.5 ± 7.83 NmL CH_4/g VS, which was low compared with the literature, usually ranging between 260 and 450 NmL CH_4/g VS depending on the fruit type, maturity stage, and process conditions, with higher yields associated with sugar-rich fruits in well-buffered environments [52,53]. The low result obtained in this study was not due to poor fruit biodegradability but rather to the inhibition of methanogenesis caused by reactor acidification and an excess of VFAs. Initial hydrolysis and acidogenesis were too fast, and the methanogens could not develop properly. Figure 2 illustrates the cumulative CH_4 production over the 20-day period of the BMP test, comparing both substrates with the control reactors.

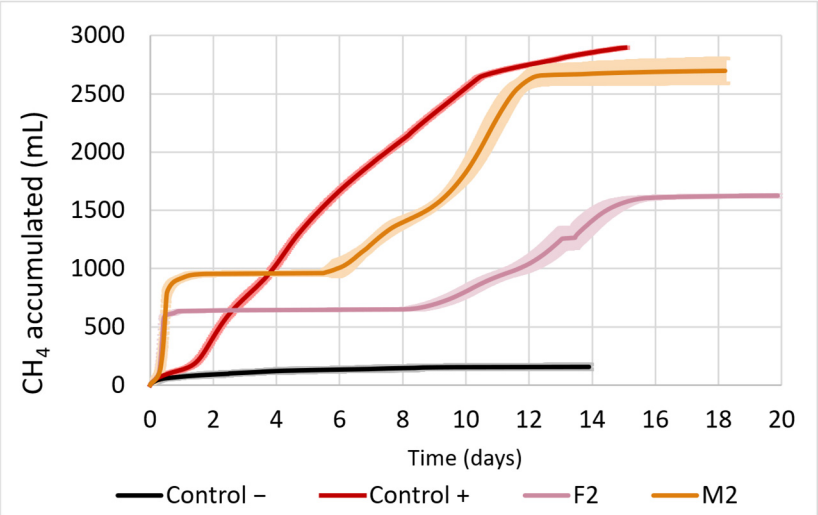

Figure 2. Accumulated CH_4 production for BMPs employing ratio I/S 2. Comparison between control (−) (only inoculum in black), control (+) (inoculum and cellulose macrocrystalline in red), molasses (M2 in orange), and fruits (F2 in pink).

The initial and final characterisation data of the tested mixtures are summarised in Table 4. At the beginning of the experiment, several parameters indicated an unfavourable starting condition for AD. The pH was notably low (particularly in fruit reactors, 5.63), whereas optimal AD performance typically occurs near neutral pH [54,55]. In addition, the VFA/Alkalinity ratios were elevated, reaching 0.80 in the molasses and 0.74 in the fruit mixture, both approaching the threshold of process instability. Most critically, the VFA concentration in the molasses reactors exceeded the recommended safety limit of 1 g/L, signalling a high risk of organic overload at the onset of the experiment [56].

Table 4. Characterisation before and after the BMP experiment for an I/S ratio of 2.

	Molasses Initial	Molasses Final	Fruit Initial	Fruit Final
pH	6.36 ± 0.05	8.17 ± 0.1	5.63 ± 0.16	7.71 ± 0.03
NH_4-N (mg/L)	1167 ± 33	1520 ± 58	1130 ± 29	1155 ± 32
COD (g/L)	36.43 ± 3.33	18.65 ± 0.9	29.3 ± 0.58	16.03 ± 0.2

C/N	16.83 ± 0.24	8.12 ± 0.08	17.06 ± 0.35	9.07 ± 0.24
TS (g/L)	34.53 ± 0.17	20.55 ± 0.07	24.29 ± 0.31	14.49 ± 0.16
VS (g/L)	27.05 ± 0.16	12.89 ± 0.04	19.93 ± 0.27	10.01 ± 0.13
VFA/Alkalinity	0.8 ± 0.03	0.51 ± 0.01	0.74 ± 0.04	0.68 ± 0.03
VFA (g/L)	5.53 ± 1.56	4.40 ± 0.1	3.95 ± 0.1	3.66 ± 0.18
Alkalinity (g $CaCO_3$/L)	6.91 ± 1.7	8.68 ± 0.2	5.33 ± 0.22	5.4 ± 0.4

By the end of the experiment, several changes could be observed. In both cases, pH increased significantly (in the M2 test, from 6.36 to 8.17, and in the F2 test, from 5.63 to 7.71), indicating the successful progression from acidogenesis to methanogenesis, with effective VFA consumption [31]. This was further supported by the decrease in the VFA/Alkalinity ratio, especially in the M2 test, which dropped from 0.8 to 0.51, a range considered favourable for stable methanogenesis. Ammonium levels increased in M2 (from 1167 to 1520 mg/L), suggesting protein degradation [44] and potential ammonia accumulation, which could be inhibitory at higher concentrations. In contrast, ammonium remained nearly constant in F2, indicating less degradation activity, coherent with lower production.

In the case of F2, it is likely that only the initial stages of AD (hydrolysis and acidogenesis) were effectively completed. These phases progressed rapidly, leading to a sharp accumulation of VFAs. As a result, methanogenesis was inhibited, and the methanogenic activity was inhibited. The imbalance between rapid acidification and delayed methanogenesis halted production [54]. This suggests that an I/S ratio of 2 was insufficient to avoid inhibition.

Both M2 and F2 showed high COD removal efficiencies (49% and 45%, respectively), indicating rapid hydrolysis and acidogenesis. However, this rapid degradation led to VFA accumulation and acidification, particularly in F2, which impaired methanogenic activity and resulted in low CH_4 yields and poor model fits. These results show that although initial degradation was effective, instability limited the overall performance.

When comparing our experimental BMP results with the Gompertz model, the previously observed conclusions were confirmed. In the case of M2 (Figure 3A), the R^2 was 0.898. These values suggest that the Gompertz model provides a reasonably good fit to the BMP curve, supported by physiologically meaningful parameters: R_{max} = 0.91 CH_4/g VS/d, λ = 0, and $G_{(0)}$ = 394 mL CH_4/g VS.

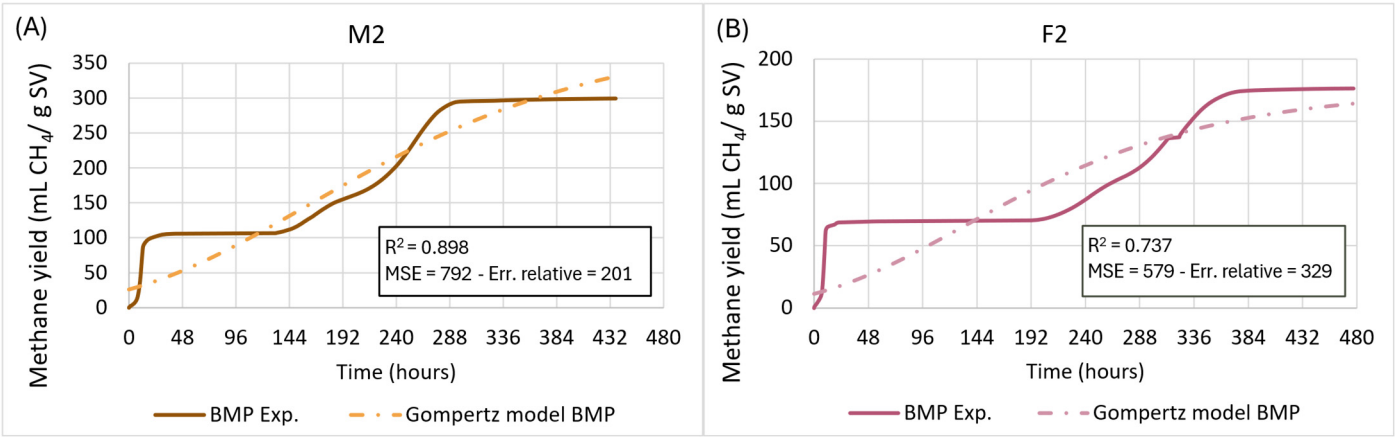

Figure 3. A comparison between the experimental BMPs at an I/S ratio of 2 with the Gompertz model. (**A**) Molasses: in dark orange, the experimental BMP; in light orange, the model. (**B**) Fruit mix: in dark pink, the experimental BMP, in light pink, the model.

In comparison with the M2 test, the results obtained for F2 show a weaker fit to the Gompertz model (Figure 3B). Both substrates yielded a rapid onset of CH_4 production ($\lambda = 0$). However, F2 had higher R_{max} (0.5 CH_4/g VS/d in M2 and 0.91 CH_4/g VS/d in F2) and lower $G_{(0)}$ (176 mL CH_4/g VS). Also, the fruit mixture displayed a lower R^2 of 0.737, in contrast to the molasses test. This suggests that despite having similar kinetic potential, the CH_4 production curve for the fruit mixture is captured worse by the Gompertz model, potentially due to more complex or variable digestion dynamics associated with the substrate's composition.

Based on the results obtained at an I/S ratio of 2, which showed instability and a tendency towards acidification, it was decided to significantly increase the I/S ratio, consistent with previous studies. Although the BMP results for M2 fell within the expected range reported by other studies, they still presented a notable risk of acidification during long-term operation, evident in the predictive model outputs, which did not suggest a stable digestion process over time. Furthermore, the literature shows that higher BMP values have been achieved for molasses substrates under higher I/S ratios [42,43]. In the case of F2, symptoms of methanogenesis inhibition were clearly observed, likely due to the accumulation of VFAs. Increasing inoculum proportion is necessary to ensure that VFAs are adequately processed during the acidogenic phase and supports stable methanogenic activity. The ratio was not increased further, as values above 4 would result in substrate concentration in terms of mg of VS too low to be reliable.

I/S Ratio of 4

The average BMP recorded for molasses (test M4) was 262.9 ± 1.49 NmL CH_4/g VS, falling within the range reported in the literature [42,43]. The average BMP for the fruit mix (test F4) was 292.8 ±6.43 NmL CH_4/g VS, which was consistent with values reported in the literature [52,53]. Compared to the I/S ratio of 2, the fruits performed significantly better, while the molasses showed a similar performance. Figure 4 presents the accumulated CH_4 over the 20-day period of BMP tests compared to the control reactors.

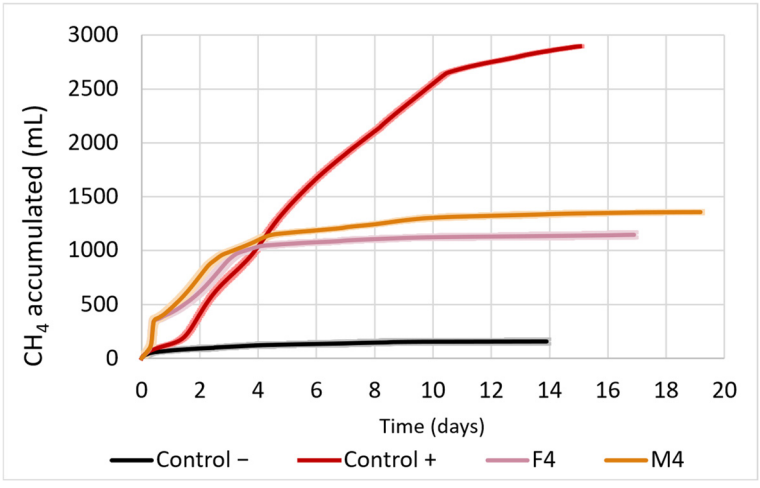

Figure 4. Accumulated CH_4 production for BMP tests employing I/S ratio of 4. Comparison between control (−) (only inoculum in black), control (+) (inoculum and cellulose microcrystalline in red), molasses (M4 in orange), and fruits (F4 in pink).

The initial and final characterisation data of the tested mixtures are detailed in the Table 5. At the start of the experiment, both M4 and F4 tests showed slightly acidic pH values of 6.63 and 6.46, respectively. While not extremely low, such pH levels can decrease the activity of methanogenic bacteria, which are crucial for CH_4 production. Moreover, ammonia concentrations in M4 (1457 mg/L) and F4 (1363 mg/L) tests are relatively high,

which could become toxic to methanogenic microorganisms at low pH by increasing the levels of free ammonia. The VFA/Alkalinity ratio is also concerning, with M4 at 0.77 and F4 at 0.85, suggesting potential acidification. The initial alkalinity values (7.53 g/L for M4 and 5.93 g/L for F4) are relatively low, which may not be adequate to buffer against the excess VFAs and prevent acidification, leading to process instability, especially in the case of fast initial degradation. [30]

Table 5. Characterisation before and after the BMP experiment for an I/S ratio of 4.

	Molasses Initial	Molasses Final	Fruit Initial	Fruit Final
pH	6.63 ± 0.05	7.93 ± 0.01	6.46 ± 0.05	7.8 ± 0.04
NH_4-N (mg/L)	1457 ± 25	1606 ± 39	1363 ± 45	2027 ± 9
COD (g/L)	34.86 ± 1.96	26.09 ± 0.29	33.17 ± 4.6	19.16 ± 01.04
C/N	17.26 ± 0.79	10.45 ± 0.4	16.96 ± 2.05	9.45 ± 0.16
TS (g/L)	33.97 ± 0.18	26.38 ± 0.27	25.06 ± 0.03	19.01 ± 0.28
VS (g/L)	25.16 ± 0.16	17.63 ± 0.08	19.14 ± 0.1	13.29 ± 0.19
VFA/Alkalinity	0.77 ± 0.04	0.51 ± 0.01	0.85 ± 0.29	0.53 ± 0.05
VFA (g/L)	5.73 ± 0.24	5.04 ± 0.3	4.53 ± 0.02	3.5 ± 0.02
Alkalinity (g $CaCO_3$/L)	7.53 ± 0.72	9.381 ± 0.4	5.93 ± 1.7	6.65 ± 0.6

Both M4 and F4 tests showed improved stability compared to the previous ones conducted at a ratio of 2. For both substrates, the final pH values rose to around 7.8–7.9, reflecting a near-neutral, slightly alkaline environment favourable for methanogenic activity. Importantly, the VFA/Alkalinity ratios dropped below the critical threshold of 0.8 (to 0.51 for M4 and 0.53 for F4), suggesting that higher inoculum proportion mitigated acidification risk. Additionally, ammonium concentrations increased, especially in F4 (up to 2027 mg/L), though not to inhibitory levels. These results demonstrate that increasing the I/S ratio not only improves process stability but also supports more complete degradation of organic matter. Nevertheless, while performance improved, the relatively high residual VFA levels (especially in M4) suggest that some acid accumulation still occurred, and further optimisation may be required to ensure robustness during long-term operation.

Compared with M2 and F2, increasing the I/S ratio to 4 resulted in lower COD removal for molasses (M4 tests, 25%) and moderately lower for fruit (F4 test, 41%), but the process was considerably more stable. This stability led to a more efficient methanogenesis, particularly in F4, which achieved the highest BMP and was best fitted by the Gompertz model. These findings suggest that COD removal alone is not a sufficient indicator of process efficiency, especially for long-term operation.

When comparing M4 results with the modified Gompertz model with the optimised parameters (R_{max} = 3.01 mL CH_4/g VS/d, λ = 0 h, and $G_{(0)}$ = 260.08 mL CH_4/g VS), the model yielded an R^2 of 0.921, indicating a reasonably good fit between the experimental and predicted curves (Figure 5A). R_{max} was substantially higher in M4 (3.01 mL CH_4/g VS/d) than in M2 (0.91 mL CH_4/g VS/d), suggesting that the microbial activity and CH_4 generation rate were markedly improved under the higher I/S. Although $G_{(0)}$ was higher in M2 (394 mL CH_4/g VS) than in M4 (260.08 mL CH_4/g VS), the rate at which M4 produced CH_4 was higher. These results suggest that while M2 may have higher biomethane yield potential, its kinetics are slower and more variable than M4. The more regular kinetics observed in M4 could be a positive indicator of robustness, warranting further validation at the reactor scale.

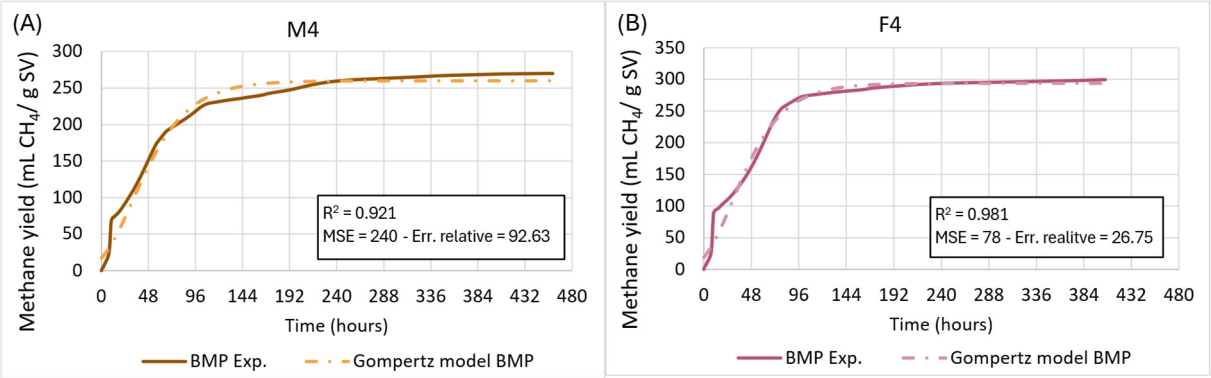

Figure 5. A comparison between the experimental BMP at an I/S ratio of 4 with the Gompertz model. (**A**) Molasses: in dark orange, the experimental BMP; in light orange, the model. (**B**) Fruit mix: in dark pink, the experimental BMP; in light pink, the model.

In test F4 (R_{max} = 3.74 mL CH_4/g VS/d, λ = 0 h, and $G_{(0)}$ = 293.74 mL CH_4/g VS), the model showed a very strong fit with the experimental data, with a high R^2 (0.981) and a low MSE (78) (Figure 5B). Moreover, the R_{max} (3.74 mL CH_4/g VS/d) was over four times higher than in F2, reflecting much more favourable microbial kinetics. This sharp increase in R_{max} suggests that the higher I/S ratio provided a more balanced microbial environment, reducing the risk of acidification and allowing methanogens to thrive. The CH_4 potential was also much higher ($G_{(0)}$ = 293.74 mL CH_4/g VS), in line with the literature. The digestion curve showed a rapid exponential phase followed by a defined plateau, indicating complete substrate conversion and metabolic stability. Compared to previous assays (F2, R^2 = 0.737), this result confirms that increasing the I/S ratio substantially improved process stability and predictability, likely due to better VFA management and enhanced methanogenic activity.

3.2.2. Co-Digestion of Fruits and Molasses

Based on these results and with the aim of treating both substrates under conditions most likely to ensure successful digestion, a co-digestion trial was designed using an I/S ratio of 4. The mixture consisted of 75% fruit waste (identified as the more promising substrate) and 25% beet molasses, allowing for an evaluation of synergistic effects under optimal inoculum conditions. Moreover, to decrease the risk of acidification and inhibition due to high ammonium content, the mixture was diluted 1:1 with water.

The total accumulated CH_4 was 520.50 ± 58.9 mL, yielding a BMP of 441.54 ± 45.98 mL CH_4/g VS. This BMP was higher than that obtained from any of the individual digestion of both substrates and surpasses the weighted average value estimated from the individual BMP results of 284.5 mL CH_4/g VS. The initial and final characterisation data of the reactors are detailed in Table 6.

Table 6. Characterisation of the reactors before and after the BMP experiment for the co-digestion of molasses and the fruit mix.

	Initial	Final
pH	6.99 ± 0.02	7.49 ± 0.02
NH_4-N (mg/L)	525 ± 10	1537 ± 12.5
COD (g/L)	20.15 ± 0.86	37.33 ± 0.28
C/N	10.78 ± 2.76	23.75 ± 1.15
TS (g/L)	17.72 ± 0.97	15.18 ± 0.22
VS (g/L)	11.79 ± 0.66	10.08 ± 0.07
VFA/Alkalinity	0.83 ± 0.01	0.28 ± 0.01

VFA (g/L)	2.6 ± 0.8	0.22 ± 0.01
Alkalinity (g $CaCO_3$/L)	2.14 ± 0.65	0.78 ± 0.03

At the beginning of the experiment, the system showed conditions generally favourable for AD. The initial pH was close to neutrality (6.99 ± 0.02), and the VFA concentration (2.6 ± 0.8 g/L) was relatively low. Although the VFA/Alkalinity ratio (0.83 ± 0.01) initially exceeded the commonly recommended threshold (0.3–0.4), the low absolute VFA concentration and sufficient initial alkalinity (2.14 ± 0.65 g $CaCO_3$/L) buffered the system effectively, preventing acidification. This is confirmed by the final pH, which increased to 7.49 ± 0.02 and is within the optimal range for methanogenic activity. Importantly, the VFA/Alkalinity ratio dropped significantly by the end of the process (to 0.28 ± 0.01), confirming that the system recovered from the initial acidogenic phase and achieved stable methanogenesis. The very low final VFA concentration (0.22 ± 0.01 g/L) further supports this conclusion.

The COD increased from 20.15 ± 0.86 g/L to 37.33 ± 0.28 g/L, likely reflecting the accumulation of intermediate soluble compounds as part of the digestion process. Meanwhile, TS and VS concentrations slightly decreased, indicating effective organic matter degradation.

Overall, the co-digestion conditions enabled a rapid and stable CH_4 production process (Figure 6A). The high R^2 value (0.9941) from the Gompertz model fitting (Figure 6B) indicates excellent agreement between experimental and predicted CH_4 production. The optimised kinetic parameters (R_{max} = 212.99 mL CH_4/g VS/d, λ = 0, and $G_{(0)}$ = 553.52 mL CH_4/g VS) further confirm a rapid onset and sustained production rate, reinforcing the superior performance of the co-digestion strategy.

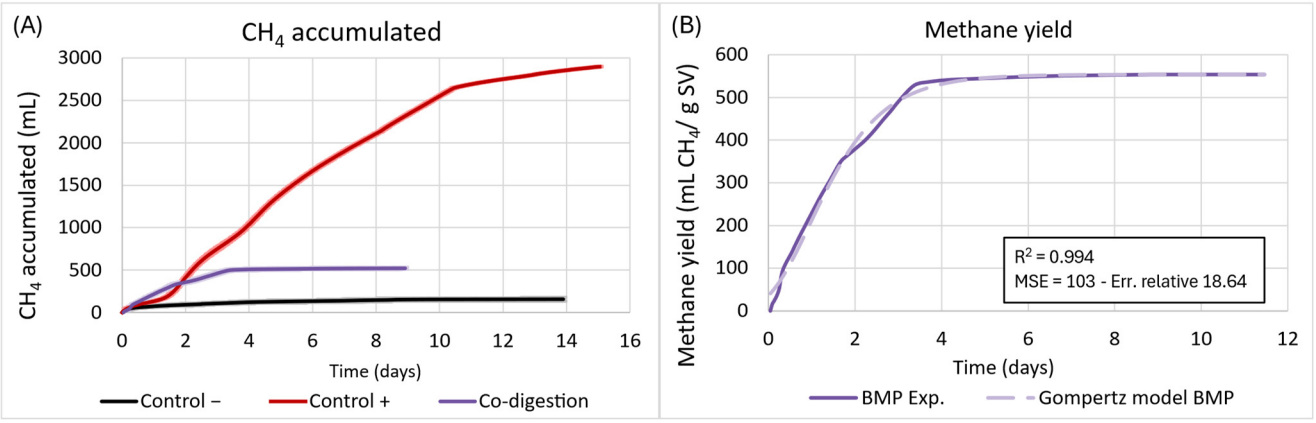

Figure 6. Co-digestion results. (**A**) Accumulated CH_4 for an I/S ratio of 4. A comparison of the control (−) (only inoculum in black), the control (+) (inoculum and cellulose microcrystalline in red), and the co-digestion I/S of 4 (in purple). (**B**) A comparison between the experimental BMP (dark purple) with its Gompertz model (light purple).

Comparing the co-digestion results to those of the individual substrates, the absence of a lag phase (λ = 0) indicates a generally quick adaptation of the inoculum, but the co-digestion achieved a remarkably high R_{max} of 212.99 mL CH_4/g VS/d, vastly exceeding the values seen in M2 (0.91), F2 (0.91), M4 (3.01), and even F4 (3.74). That suggests a significantly enhanced CH_4 production rate, likely due to improved substrate balance and synergistic effects. Moreover, the $G_{(0)}$ value of 553.52 mL CH_4/g VS outperformed all mono-digestion setups. Overall, the co-digestion configuration demonstrated a clear synergistic effect and provided the most robust and kinetically favourable conditions, making it the most suitable option for implementation in the scaled-up reactor.

3.3. Scaled-Up Operation

Based on the BMP results, a 6 L anaerobic digester was operated using the optimal substrate mixture (S0). However, the process faced instability due to acidification caused by the rapid degradation of sugars and insufficient buffering capacity. To counteract this, three mitigation strategies were tested sequentially: (S1) carbonate addition, (S2) biochar supplementation, and (S3) the integration of BES. Table 7 shows the feed characterisation of each phase and Table 8 the differences in the physicochemical parameters before and after applying the different solutions.

Table 7. Characterisation of the different feeds of the scale-up reactor.

	S0	S1	S2 and S3
pH	5.07 ± 0.4	6.30 ± 1.4	7.45 ± 1.37
Conductivity (mS/cm)	13.12 ± 3	17.53 ± 1.9	19.93 ± 1.1
COD total (g/L)	89.86 ± 4.5	77.97 ± 3.1	92.01 ± 8.1
COD soluble (g/L)	89.44 ± 4.2	76.67 ± 1.9	86.43 ± 7.7
NH_4-N (mg N/L)	41.5	41.28 ± 11	57 ± 23
TN (mg N/L)	1943 ± 769	1106 ± 93	1163 ± 288
TS (g/L)	134.4 ± 38	70.33 ± 6.1	84.39 ± 10
VS (g/L)	117.9 ± 43	46.69 ± 4.6	59.09 ± 8.3
Alkalinity (mg $CaCO_3$/L)	658 *	3393 ± 1376	6431 ± 2467
VFA/Alkalinity	7.24 *	3.96 ± 2.75	0.84 ± 0.3
VFA (mg/L)	8057 *	9190 ± 2847	6485 ± 871
Ratio C/N	51.11 ± 18	71.01 ± 8.1	83.45 ± 21

S0: 75% fruits + 25% molasses, diluted 1:1 water and filtered 2 × 2 mm mesh—organic loading rate (OLR) = 2.995 kg COD/m^3/day. **S1:** S0 + 10 g/L Na_2CO_3 − OLR = 2.605 kg COD/m^3/day. **S2:** S1 + 10 g/L biochar − OLR = 3.07 kg COD/m^3/day. * The pH was too acid, and the values of the replicates were outside the range.

Table 8. The analysis of the AD digestate before and after applying the different solutions.

	Solution S1		Solution S2		Solution S3	
	Before	After	Before	After	Before	After
pH	6.74 ± 1.1	6.46 ± 0.3	6.67 ±0.3	6.20 ± 0.2	7.2	6.29 ± 0.5
Conductivity (mS/cm)	27.24 ± 5.2	28.70 ± 1.3	29.14 ± 0.9	27.90 ± 1.6	27.90 ± 1.6	23.06 ± 3
COD total (g/L)	56.02 ± 3.81	68.52 ± 2.6	65.09 ± 1.8	71.40 ± 3.2	71.40 ± 3.2	66.97 ± 7.6
COD soluble (g/L)	55.48 ± 4.1	63.05 ± 2.3	62.56 ± 1.7	63.19 ± 4.5	63.19 ± 4.5	60.79 ± 7
NH_4-N (mg N/L)	834 ± 492	677 ± 115	55 ± 16	84 ± 10	84 ± 10	56 ± 23
TN (mg N/L)	1293 ± 405	1230 ± 90	1170 ± 239	1332 ± 163	1332 ± 163	1212 ± 55
TS (g/L)	101.5 ± 12	65.27 ± 10	59.57 ± 5.2	63.36 ± 2.3	63.36 ± 2.3	52.58 ± 6.9
VS (g/L)	77.53 ± 10	37.60 ± 10	33.80 ± 4.6	37.42 ± 1.6	37.42 ± 1.6	30.04 ± 4.8
Alkalinity (g $CaCO_3$/L)	9.43 ± 0.4	8.13 ± 1.3	8.60 ± 0.9	6.08 ± 1.2	6.08 ± 1.2	5.90 ± 1.4
VFA/Alkalinity	2.14 ± 0.7	3.42 ± 0.5	2.91 ± 0.3	3.57 ± 0.5	3.57 ± 0.5	3.18 ± 0.4
VFA (g/L)	23.65 ± 2.1	27.26 ± 1.83	24.90 ± 1.9	21.93 ± 5.6	21.93 ± 5.6	18.35 ± 3
Ratio C/N	46.23 ± 19	56.08 ± 5.6	56.46 ± 12	66.37 ± 26	66.37 ± 26	55.5 ± 8.5

3.3.1. Baseline Operation (S0)

During the first four weeks, the reactor was fed with a 1:1 water-diluted mixture of fruits and molasses (S0). As shown in Table 7, the feed exhibited very low pH (5.07 ± 0.4), minimal alkalinity (658 mg/L $CaCO_3$), and high VFA concentration (8057 mg/L), resulting in an excessively VFA/Alkalinity ratio (7.24), well above the stability threshold. These conditions favoured acidogenic bacteria, which rapidly converted the available sugars into

VFAs. Despite manual pH corrections using NaOH, the outlet measurements indicated persistent acidification and poor buffering capacity, impairing the reactor's ability to maintain suitable conditions for methanogenesis (Table 8).

CH_4 production during S0 was limited and heavily reliant on external pH control. As shown in Figure 7, the maximum CH_4 yield was 0.46 L CH_4/L/d. Given an OLR of 3.93 g VS/L/day, the resulting specific CH_4 yield was 117.04 mL CH_4/g VS/day. This value corresponds to approximately 55% of the maximum CH_4 production rate (R_{max}) of 212.99 mL CH_4/g VS/day observed in the BMP co-digestion assay under ideal batch conditions. This reduced yield aligns with expected differences between batch and continuous systems, compounded by unstable pH conditions. The biogas composition was initially dominated by CO_2 (70%) and H_2 (26%), with only 4% CH_4, indicating a system dominated by hydrolytic and acidogenic activity (Figure 8). Although temporary CH_4 improvements were observed after pH stabilisation, these were not sustained. The reactor demonstrated clear signs of acid regression, confirming that the initial substrate composition was too destabilising for long-term AD performance without buffering enhancement. The average calorific value of biogas was 7.16 MJ/m^3.

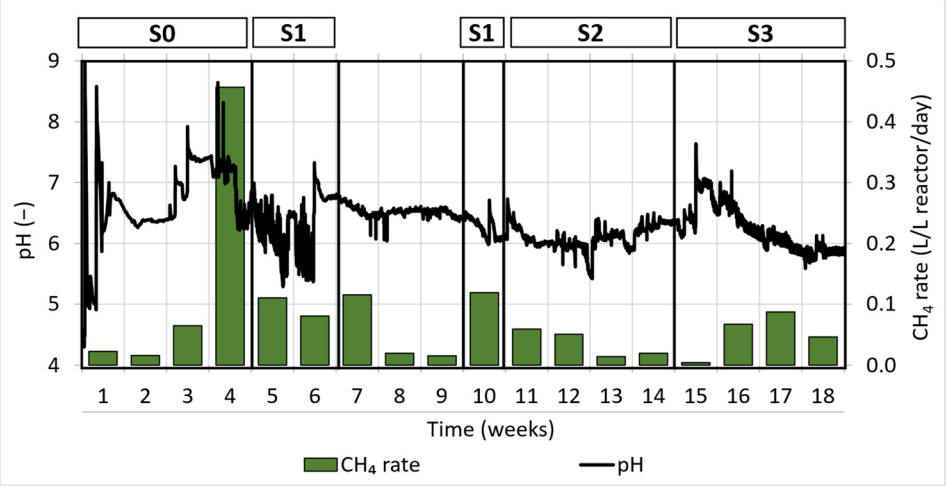

Figure 7. Biogas production vs. pH. In the left axis, the pH monitored continuously every 15 min; in the right axis, the average CH_4 production per week (L/L reactor/day). S0 is the operation with manual pH adjustments with NaOH, S1 is feeding amended with Na_2CO_3 10 g/L, S2 is S1 amended also with biochar 10 g/L, and S3 is the operation with S2 and the BES reactor in the recirculation loop.

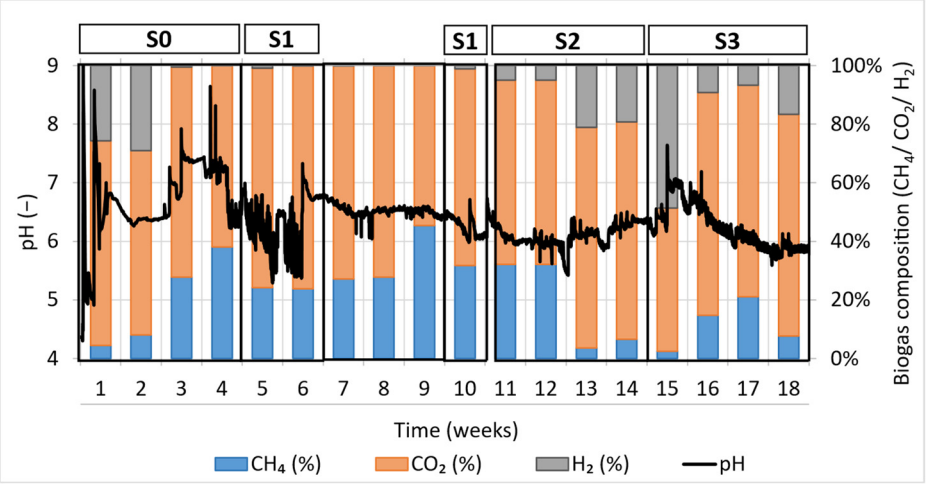

Figure 8. Biogas composition. In the left axis, the pH monitored continuously each 15 min; in the right axis, the average biogas composition per week. S0 is the operation with manual pH adjustments with NaOH, S1 is feeding amended with Na_2CO_3 10 g/L, S2 is S1 amended also with biochar 10 g/L, and S3 is the operation with S2 and the BES reactor in the recirculation loop.

Strategy 1: Carbonate Addition (S1)

To enhance buffering, 10 g/L of Na_2CO_3 was added to the feed during weeks 5–10. This amendment increased the initial feed pH (from 5.07 ± 0.4 to 6.30 ± 1.4) and raised alkalinity (from 658 to 3393 ± 1376 mg/L) (Table 7), partially neutralising the acidic nature of the fruit/molasses mixture. Despite these improvements, Table 8 shows that the VFA/Alkalinity ratio increased over time (from 2.14 ± 0.7 to 3.42 ± 0.5), and VFA concentrations remained high. This indicated that acidogenic activity continued to dominate, overwhelming the added buffering capacity.

As shown in Figure 7, CH_4 production remained unstable. A temporary recovery was observed after a three-week feeding pause (weeks 6–9), which was meant to allow for methanogens to metabolise the accumulated VFAs. However, CH_4 production declined rapidly once feeding resumed. Biogas composition during this phase (Figure 8) showed CH_4 values around 24–32% and fluctuating H_2 levels, indicating that methanogenesis was not fully re-established. The calorific value of the biogas ranged between 8.59 and 11.45 MJ/m^3. Based on the analytical data showing insufficient alkalinity, a declining pH unable to remain stable, and low and decreasing production, S1 is considered to have failed in stabilising the reactor.

The addition of Na_2CO_3 in strategy S1 temporarily improved the feed's pH and alkalinity; however, it was insufficient to counteract the high acidogenic pressure generated by the rapid fermentation of sugars in the fruit/molasses mixture. Although initial alkalinity increased fivefold compared to the baseline, the VFA/Alkalinity ratio at the outlet remained well above the stability threshold reported in the literature (> 0.3–0.4), reaching values above 3.4. This indicates that the rate of VFA generation exceeded the buffering capacity provided by carbonate addition. Similar findings have been reported in systems treating highly biodegradable, sugar-rich residues, where chemical buffering alone could not restore methanogenic activity without reducing organic loading or improving C/N balance. In this study, the persistently high C/N ratio (> 50) and OLR (~2.6 kg COD/m^3·day) favoured acidogenic over methanogenic communities, leading to sustained accumulation of VFAs despite the increased alkalinity. Consequently, Na_2CO_3 addition delayed but did not prevent acidification, confirming that chemical pH correction, without addressing the underlying substrate imbalance, is insufficient for long-term stability in the co-digestion of these residues. In real field applications, this limitation would be even more critical since the kinetic dissolution of shell-derived $CaCO_3$ is slower than that of Na_2CO_3, further reducing its effectiveness in counteracting acidification.

Strategy 2: Biochar Addition (S2)

In weeks 11–14, biochar (10 g/L) was added alongside Na_2CO_3 to the feed. This increased the initial pH (7.45 ± 1.37) and alkalinity (6431 ± 2467 mg/L), as shown in Table 7. Biochar also reduces the VFAs (6485 mg/L), potentially by adsorbing organic acids and offering surfaces for microbial colonisation. However, outlet values indicated persistent instability (Table 8). The VFA/Alkalinity ratio remained high at 3.57 ± 0.5, and outlet pH averaged 6.20 ± 0.2, reflecting conditions still unfavourable for methanogenesis.

CH_4 production steadily declined throughout this phase, falling 0.01 L CH_4/L/day by week 14 (Figure 7). Biogas composition showed a shift away from methanogenesis, with H_2 levels increasing from 5% to 19% and CH_4 dropping from 32% to 7% (Figure 8). The increasing presence of H_2 indicates a predominance of acidogenic bacteria, with poor CH_4

conversion despite improved feed parameters. The average calorific value of biogas in this phase was 6.8 MJ/m^3. Although the pH appeared to be better maintained, it remained unstable, while biogas production reached its lowest point and was accompanied by a significant increase in H_2. Therefore, S2 also failed to stabilise the reactor.

Despite improving influent characteristics and mitigating acid peaks, biochar addition failed to suppress acidogenesis or restore methanogenesis, as shown by high VFAs, low pH, and declining CH_4 yields, with an average calorific value of 6.8 MJ/m^3 during this phase. Its limited effectiveness can be attributed to its primarily physical mode of action: while the porous structure can temporarily adsorb VFAs and provide microbial attachment sites, it lacks the intrinsic chemical buffering capacity needed to neutralise acids at the rate generated from the highly biodegradable fruit/molasses mixture. The rapid acid accumulation exceeded biochar's adsorption capacity, and the uncorrected C/N imbalance further favoured acidogenic over methanogenic populations. Consequently, without lowering the organic loading rate or co-digesting with substrates offering greater buffering potential, biochar alone was insufficient to achieve long-term process stability.

Strategy 3: Bioelectrochemical System Integration (S3)

During weeks 15–18, a BES was incorporated into the reactor's recirculation loop. Prior to integration, the pH was manually adjusted to 7.2 to prevent biofilm collapse. This phase used the same feed as in S2, meaning input conditions were consistent (Table 7). Initially, the outlet parameters showed moderate improvements: COD removal slightly increased, VFA concentration decreased to 18.35 g/L, and the VFA/Alkalinity ratio decreased to 3.18 ± 0.4 (Table 8). However, as the phase progressed, pH (6.29 ± 0.5) and alkalinity (5.90 ± 1.4) declined again, impairing BES performance and ultimately leading to a collapse in the reactor.

The BES integration initially showed promising results, with CH_4 production rising to 0.09 L CH_4/L/day by week 17 (Figure 7). Biogas quality also improved during this phase (Figure 8), with CH_4 content rising to 21% and H_2 levels decreasing to 7–9%. The specific CH_4 yield was 45.69 mL CH_4/g VS/day, approximately 21.5% of the R_{max} (212.99 mL CH_4/g VS/day) observed under batch conditions. However, these improvements were not sustained. By week 18, acidification recurred, inhibiting both methanogenic and electroactive microbial communities. The average calorific value of the biogas during this phase was 3.94 MJ/m^3. Although the BESs initially improved reactor performance, increasing both biogas production and CH_4 content while reducing H_2 levels, they did not improve pH stability, which ultimately led to reactor collapse due to acidification. Thus, despite the initial benefits, S3 is also considered to have failed in stabilising the reactor in the long term.

The failure of the BES integration can be primarily attributed to the acidification of the reactor environment, which negatively affected the growth and activity of the electroactive microbial communities essential for biofilm formation and electron transfer. The low pH conditions disrupted the metabolism of key electrogenic bacteria, leading to a decline in current production and CH_4 yield. The unstable electrochemical behaviour observed in the BES cells, including shifts in electrode potentials and the loss of biofilm activity, is discussed in greater detail in 3.3.2. BES Performance. Overall, these factors resulted in the inability of the BES to maintain enhanced performance in long-term operation.

Key Findings and Limitations

As evidenced by the evolution of feed and outlet parameters (Tables 7 and 8) and biogas trends (Figures 7 and 8), none of the tested mitigation strategies were able to achieve long-term stability in the reactor. Although all approaches (carbonate addition,

biochar supplementation, and BES integration) contributed to temporary improvements in buffering and CH_4 production, these effects were insufficient to overcome the rapid acidification induced by the feedstock.

Na_2CO_3 addition temporarily improved pH and alkalinity but was insufficient to counterbalance the rapid acid generation driven by the sugar-rich, nitrogen-deficient substrate. Biochar supplementation increased alkalinity and reduced VFAs in the feed; however, it failed to prevent acid accumulation or restore stable methanogenesis due to its limited chemical buffering capacity.

BES integration yielded the highest short-term gains in CH_4 production and biogas quality, but its performance was highly sensitive to pH. Acidification eventually disrupted the electroactive biofilm and electron transfer processes, leading to reactor performance decline. The detailed electrochemical behaviour of the BES system is discussed in Section 3.3.2.

Overall, the substrate (rich in sugars and low in nitrogen) requires additional stabilisation measures. Future work should explore lowering the organic loading rate, increasing hydraulic retention time, or co-digesting with substrates like animal manure that contribute buffering capacity and a more balanced C/N ratio. Without such modifications, long-term AD of these residues under rural Ghanaian conditions remains challenging.

3.3.2. BES Performance

The inoculation of the BES module took place over six days at a working voltage of 0.3 V and two days at 0.4 V. On day 8, the cells were integrated into the recirculation loop of the AD reactor. Two cells (Cell 1 and Cell 2) were prepared and operated in the same way during inoculation. However, as shown in Figure 9, Cell 2 did not produce current at any point, neither during inoculation nor during operation.

In contrast, Cell 1 showed a gradual increase in current during the inoculation week. From days 4 to 8, the BES cells were fed with S2 instead of acetate medium to transition towards the composition of the main reactor prior to the integration of both reactors. On day 7, the pH dropped to 6.1, negatively impacting the current because the medium had transitioned to being predominantly S2, displacing acetate medium as the main component. The current slightly recovered when the working voltage was increased to 0.4 V but did not sustain when the cells were integrated into the reactors.

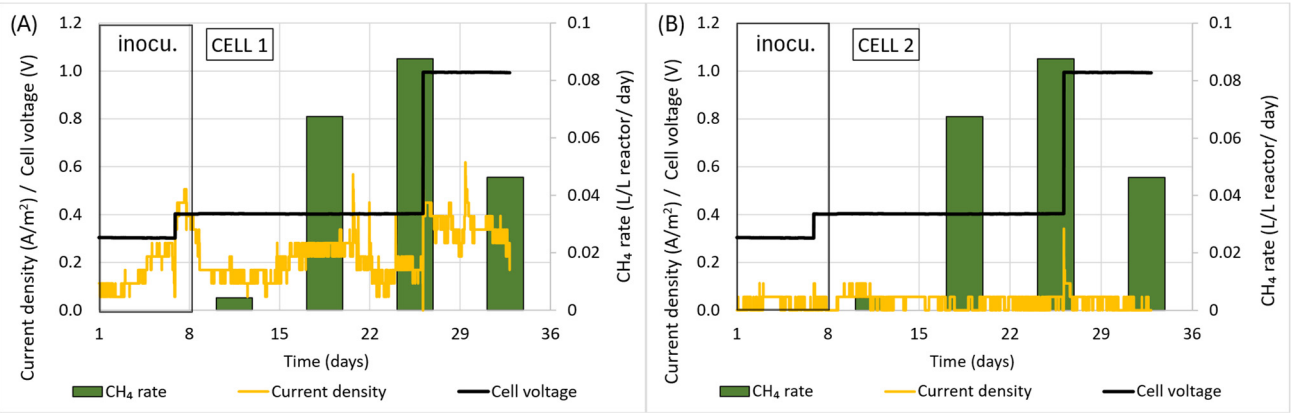

Figure 9. Current production and CH_4 production during S3. In the left axis, the current density (A/m^2) and the cell voltage (V); in the right axis, the average CH_4 production per week (L/L reactor/day). The left graph (**A**) corresponds to Cell 1, and the right graph (**B**) corresponds to the Cell 2.

The integration on day 8 led to a decrease in current from 0.5 A/m^2 to 0.18 A/m^2. This sudden change was due to the shift in composition within the BES cells, which transitioned from working with a mix of acetate medium and S2 to handling the higher organic

load introduced from the AD reactor. The AD reactor medium was rich in COD (71.4 g/L of COD, primarily VFAs and simple sugars) and had greater acidity (pH of 6.2).

During the first week with S3 (days 8–15), both the current and biogas production remained low. In the second week (days 16–22), the current rose slightly to ~0.3 A/m², coinciding with increased CH_4 production. However, in the third week, the current declined despite continued biogas growth, likely due to pH acidification weakening the electroactive biofilm.

To stimulate microbial metabolism and increase the electrode demand, the working voltage was raised to 1 V. This caused a sudden spike in current, but the increase was solely due to the abrupt voltage change and was not sustained over time. CH_4 production stayed stable initially but dropped the following week.

Figure 10 illustrates the evolution of electrode potentials, providing insight into biofilm formation and the type of microbial community present. During the inoculation week, both cells experienced a decrease in the anode and cathode potentials. In Cell 1, the anode potential stabilised around −0.45 V and the cathode at −0.8 V, whereas in Cell 2, the anode potential was −0.27 V and the cathode −0.67 V. Low anode potentials favour the colonisation of the electrode by anodic respiring bacteria (ARB) such as *Geobacter* sp., which use direct contact with the electrode for electron transfer. Meanwhile higher anode potentials led to a high diversity of microorganisms, including non-ARB or ARB that use electron shuttles, whose biofilm is less conductive, and avoided microorganisms like *Geobacter* sp. that interact with the electrode and form a biofilm [57]. Ideally, the anode potential should be at least around −0.4V and the cathode around −0.9 V [58]. Thus, it seems that Cell 2 was never fully inoculated.

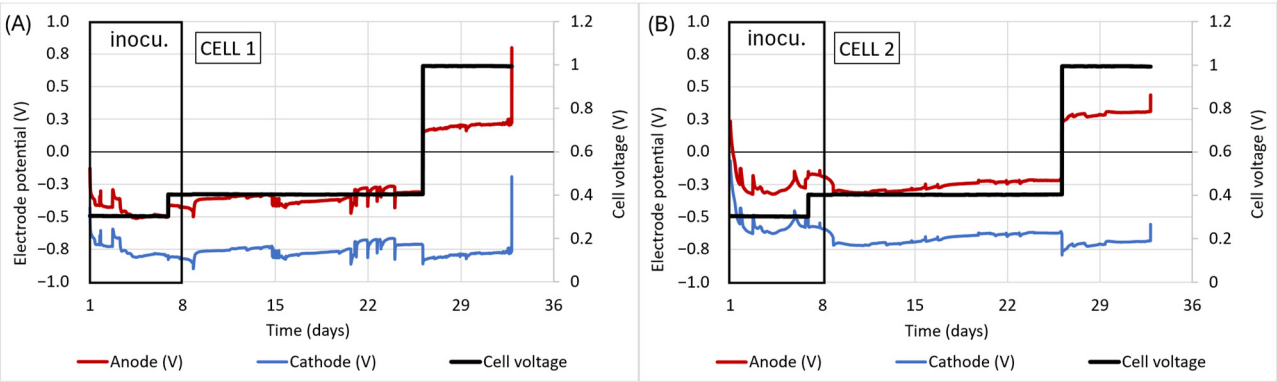

Figure 10. Cell potentials during S3 operation. In the left axis, the electrode potentials (V); in the right axis, the cell voltage (V). The left graph (**A**) corresponds to Cell 1, and the right graph (**B**) corresponds to Cell 2.

In Cell 2, the increase in the potentials remained consistent throughout the operation, resulting in values that were too high to support the development of an electroactive biofilm. Conversely, Cell 1 exhibited stabilisation of the anode potential, maintaining values below −0.5 V, though it showed an upward trend over time, indicating a constant loss of biofilm activity.

During the third S3 week (week 17 of operation), the potentials became unstable, experiencing significant fluctuations with each new feeding. These abrupt changes could have negatively impacted the biofilm. In the final week of operation, when the working voltage was increased to 1 V, the anodic potential of both cells became positive.

The failure of the BES cells can be primarily attributed to the acidification of the medium, which severely impacted the growth and activity of electroactive bacteria. Acidic conditions disrupt the metabolism of key electrogenic microorganisms such as *Geobacter* spp., which rely on direct extracellular electron transfer (EET) via conductive biofilms

attached to the anode. As the pH drops below optimal levels, typically 6.5, the microbial community structure shifts, leading to a decline in the abundance of ARB and a reduction in the formation of conductive biofilms. This is clearly reflected in the gradual decrease in current density and the concurrent shift in electrode potentials toward more positive values, particularly at the anode, indicating a loss of electrochemical activity. A positive shift in anode potential suggests that fewer electrons are being transferred to the electrode, consistent with a weakening or collapse of the biofilm. Ultimately, this cascade of effects, starting with acidification, leads to a progressive decline in system performance, both in terms of electron transfer and biogas production, marking the breakdown of the bioelectrochemical process.

3.3.3. Organic Matter Removal: COD, Total Solids, and Volatile Solids

The removal of organic matter was evaluated using COD, TS, and VS as indicators of substrate degradation and reactor efficiency. Variations across the four operational phases (S0–S3) revealed significant instability, with removal efficiency closely tied to acidification and process performance. The results are summarised in Figures 11 and 12.

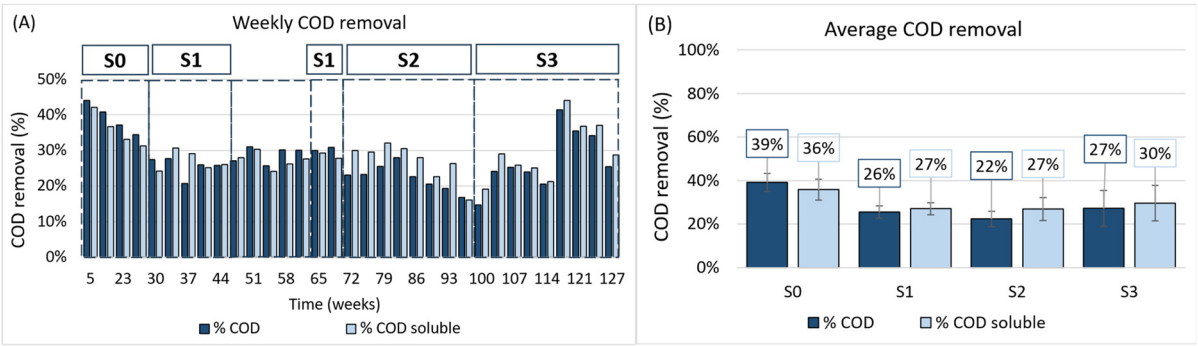

Figure 11. COD treatment. Left (**A**), the evolution of the COD removal during the 18 weeks of operation. Right (**B**), the average removal rates of each phase. S0 is the operation with manual pH adjustments with NaOH, S1 is feeding amended with Na_2CO_3 10 g/L, S2 is S1 amended also with biochar 10 g/L, and S3 is the operation with S2 and the BES reactor in the recirculation loop.

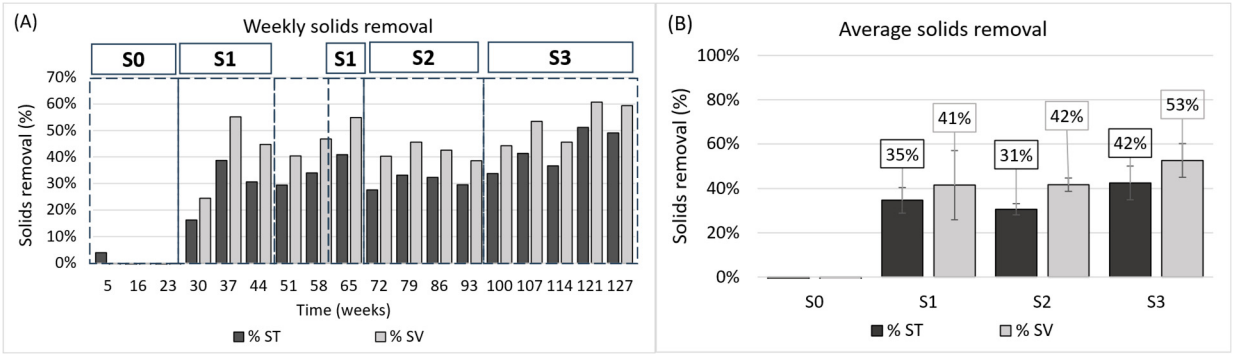

Figure 12. Total and volatile solid removal. Left (**A**), the evolution of the removal during the 18 weeks of operation. Right (**B**), the average removal of each phase. S0 is the operation with manual pH adjustments with NaOH, S1 is feeding amended with Na_2CO_3 10 g/L, S2 is S1 amended also with biochar 10 g/L, and S3 is the operation with S2 and the BES reactor in the recirculation loop.

Phase S0—Baseline

During the baseline operation (S0), COD removal efficiency was variable, ranging from 34% to 44% and showing a decrease over time. This was closely related to the instability of the reactor, which suffered from VFA accumulation and methanogenic inhibition. The partial COD removal was likely associated with acidogenic conversion of sugars to

VFAs rather than CH_4 production. These results reflect the incomplete degradation of organic matter under acidified conditions.

During the initial weeks of reactor operation, solid removal efficiencies appeared to be negative. This was because the feedstock introduced into the system contained a lower concentration of solids compared to the inoculum, which initially constituted the majority of the reactor volume. As a result, the effluent consistently exhibited higher solid content than the influent. This apparent increase in solids concentration at the outlet reflect not inefficiency but a transitional phase in which the inoculum was gradually being displaced by the substrate. Only after the reactor content had been fully renewed and stabilised under continuous feeding conditions was it possible to observe a true representation of solid degradation and removal efficiency.

Phase S1—Carbonate Addition

The addition of sodium carbonate during phase S1 resulted in a relatively stable COD removal efficiency (21–27%) throughout the period. Although Na_2CO_3 does not markedly enhance COD degradation, it contributes to maintaining process stability by buffering pH fluctuations. However, its effect appears limited under high-organic-loading conditions.

TS and VS removal during S1 exhibited a notable and rapid increase, particularly at the beginning of this phase (approximately four weeks into the operation), when the initial inoculum had been largely displaced from the reactor. This marked the point at which the solid content in the effluent more accurately reflected the degradation of the introduced substrate rather than the residual solids from the inoculum. As a result, a clearer picture of the reactor's removal efficiency emerged, with an average solid removal of 26% (TS).

Phase S2—Biochar Addition

In phase S2, the addition of biochar led to an initial increase in COD removal, from 23% to 28%. The porous structure and adsorptive capacity of the biochar likely contributed to temporary retention and partial degradation of organic compounds. However, as acidification progressed, COD removal efficiency decreased down to 17%. This pattern suggests that although biochar can buffer pH fluctuations and support microbial communities, its effects are short-lived without further system stabilisation.

Biochar did not improve TS and VS removal during the initial weeks of S2. Solid removal remained stable at 31% and 42% average for TS and VS, respectively, similar values to those in S1. These results reinforce the notion that buffering alone is insufficient to maintain consistent degradation without controlling organic overload.

Phase S3—BES Integration

With the integration of the BES, COD removal showed a modest but meaningful increase compared to earlier phases. During week 17, removal efficiency reached 41%, the highest observed in the entire operation. The presence of electroactive bacteria and enhanced electron transfer may have facilitated the partial oxidation of VFAs and other intermediates. However, as the pH dropped again in week 18, COD removal declined, underscoring the need to maintain pH stability for BES performance.

TS and VS removal rates showed a modest improvement during the initial weeks of BES operation, reaching 51% and 61%, respectively. These values suggest that the BES may have stimulated broader microbial activity, potentially enhancing the breakdown of more complex organic matter. However, the increase in removal efficiency during the final weeks did not correlate with a rise in biogas production, indicating that, in the absence of sustained environmental control, the system remained prone to acidification and microbial inhibition. Additionally, the initial improvement in solid removal may be partly due

to the physical presence of the BES electrodes, which increased surface area for solid accumulation. As such, the observed reductions may reflect physical retention rather than true biodegradation.

Synthesis and Implications

Overall, the removal of COD, TS, and VS across all phases revealed clear limitations in the stability and efficiency of the digestion process. Organic matter was only partially degraded under all tested conditions, with frequent setbacks due to acidification and microbial inhibition. Although strategies like biochar and BES provided temporary improvements, none were sufficient to ensure complete and consistent degradation of the substrate. These findings align with previous reports on AD of sugar-rich substrates, where high hydrolysis rates lead to acid accumulation and reduced CH_4 conversion efficiency. Effective control of the organic loading rate, or the introduction of complementary substrates with more favourable nutrient and buffering profiles, is essential to improve organic matter removal in such systems.

3.4. Biogas Feasibility and Challenges at Nkawie

Nkawie Senior High School (SHS) in Ghana is initiating the use of AD technology to convert organic waste into biogas, aiming to provide a sustainable energy alternative to supplement its current use of wood and LPG for cooking. The school generates a substantial amount of organic waste and can source additional waste from nearby markets, estimated at 2 metric tons of fruit waste and 500 kg of molasses per week. The findings suggest that this waste could produce approximately 86 cubic meters of biogas per week, yielding an energy output of 1978 MJ per week. However, the school's current weekly energy consumption for cooking is much higher at about 184,988 MJ, met through two truckloads of wood and 200 L of LPG (detailed calculations are provided in the Supplementary Information).

These results align with findings from similar studies in Ghana and other regions. Arthur et al. [59] investigated the biomethane potential of agricultural residues in Ghana and found that while biogas can significantly reduce dependence on traditional fuels, the energy yield often falls short of completely replacing conventional energy sources like wood and LPG. This conclusion is supported by Addae et al. [23], who examined waste disposal in Kumasi and determined that biogas production, although feasible, typically does not meet the full energy needs of large institutions like schools. Achieving full energy self-sufficiency usually requires integrating biogas systems with other renewable energy solutions and energy efficiency strategies. For example, the Africa Biogas Partnership Program found that small-scale biogas systems in East African schools and households only fulfilled a portion of their energy needs [5], underscoring the importance of supplementary energy sources. Biogas production from organic waste can vary widely depending on the substrate type, climate, and digester performance. A study by Rao et al. [60] demonstrated that co-digesting fruit and vegetable waste with animal manure produced higher CH_4 yields compared to single-substrate digestion. This finding suggests that optimisation strategies, such as co-digestion or waste pre-treatment, could enhance biogas production at Nkawie SHS, improving the system's ability to meet the school's energy requirements. Additionally, Wang et al. [61] highlighted that adjustments in the inoculum-to-substrate ratio and maintaining optimal pH and temperature conditions can significantly boost CH_4 production, approaches that Nkawie SHS could adopt to optimise its biogas system.

Despite its partial contribution to the total energy needs, the biogas system offers considerable environmental benefits. Reducing the consumption of wood and LPG could lower the school's carbon footprint and consumption of natural resources, contributing to

broader environmental sustainability goals. Additionally, decreased fuelwood usage would support local anti-deforestation efforts. Rajagopal et al. [50] emphasised the environmental benefits of biogas technology, particularly its role in reducing CO_2 emissions and mitigating deforestation in regions reliant on wood for cooking. The school could also benefit from long-term cost savings through biogas adoption. The estimated initial investment for an anaerobic digester ranges from USD 10000 to USD 50000, with annual maintenance costs of approximately USD 500 (Supplementary Information provides further details). Financial assistance or grants could help offset these costs. Over time, the investment is expected to be cost-effective due to reduced fuel expenses. The school currently spends around USD 1500 annually on refuse disposal, and biogas systems in similar settings have shown significant economic benefits, particularly in stabilising energy costs by reducing dependence on volatile fuel prices, as noted by Kadam and Panwar [62]. Nkawie SHS was advised to explore optimisation techniques such as co-digestion and substrate pre-treatment and consider integrating other renewable energy systems, like solar PV, to maximise energy output. Future studies should focus on the long-term performance of biogas systems and their integration with additional renewable energy sources to develop a comprehensive and sustainable energy solution for the school.

4. Conclusions

This study aimed to offer a practical solution for energy independence in a rural Ghanaian secondary school by evaluating the AD potential of fruit waste and beet molasses, two organic residues already available on site. Several key findings emerged:

1. Co-digestion at an I/S ratio of 4 provided the best performance, with a BMP of 441.54 ± 45.98 NmL CH_4/g VS and faster degradation compared to mono-digestion, confirming the importance of balancing the substrate load and microbial activity.
2. Fruit waste showed high sensitivity to the I/S ratio, and low inoculum loads led to acidification and inhibition, highlighting the critical role of inoculum concentration in process stability.
3. Scale-up trials revealed persistent instability, especially under high-organic-loading rates, where acidification rapidly inhibited methanogenesis despite promising BMP results.
4. Three low-cost mitigation strategies were evaluated: eggshell-derived carbonate, biochar, and BES integration. Only the BES showed a temporary improvement in CH_4 yield, but none achieved long-term stabilisation without active pH control.
5. This work demonstrates the importance of adapting AD solutions to the local context, using materials and resources that are realistically accessible in rural areas rather than relying solely on technically optimal solutions.

Future research should explore operational strategies better suited to high-strength, sugar-rich substrates, such as controlled dilution, phased feeding, or co-digestion with buffering-rich residues like animal manure. Ensuring the long-term viability of AD in low-resource settings requires both technical refinement and alignment with local economic and logistical conditions.

Supplementary Materials: The following supporting information can be downloaded at: https://www.mdpi.com/article/10.3390/su17177590/s1, Figure S1: Photo of the BMP equipment.; Table S1: Characterization of the biochar from Carbon Cycle company (2022).

Author Contributions: R.A.-S.: Conceptualisation, Methodology, Validation, Formal analysis, Investigation, Data Curation, Writing—Original Draft, S.C.: Writing—review and editing, Supervision, Methodology, Investigation, Conceptualisation, A.A.: Writing—review and editing, Formal analysis, Resources, Conceptualisation, I.B.: Writing—review and editing, Resources, Conceptualisation,

K.A.: Writing—review and editing, Resources, F.K.S.: Writing—review and editing, Resources, D.M.: Writing—review and editing, Supervision, Project administration, Resources, Funding acquisition, Conceptualisation, E.B.: Writing—review and editing, Resources, Funding acquisition, Conceptualisation. All authors have read and agreed to the published version of the manuscript.

Funding: This project SESA (Smart Energy Solutions for Africa) received funding from European Union's Horizon 2020 research and innovation programme under the grant agreement No. 101037141.

Institutional Review Board Statement: Not applicable.

Informed Consent Statement: Not applicable.

Data Availability Statement: All the experimental data are available in Zenodo (https://doi.org/10.5281/zenodo.14921811, accessed on 25 February 2025).

Conflicts of Interest: The authors have no competing interests to declare that are relevant to the content of this article.

References

1. Karimu, A. Cooking fuel preferences among Ghanaian Households: An empirical analysis. *Energy Sustain. Dev.* **2015**, *27*, 10–17. https://doi.org/10.1016/j.esd.2015.04.003.
2. Karimu, A.; Mensah, J.T.; Adu, G. Who Adopts LPG as the Main Cooking Fuel and Why? Empirical Evidence on Ghana Based on National Survey. *World Dev.* **2016**, *85*, 43–57. https://doi.org/10.1016/j.worlddev.2016.05.004.
3. Mensah, J.T.; Marbuah, G. Amoah A Energy demand in Ghana: A disaggregated analysis. *Renew. Sustain. Energy Rev.* **2016**, *53*, 924–935. https://doi.org/10.1016/j.rser.2015.09.035.
4. Lohani, S.P.; Havukainen, J. Anaerobic Digestion: Factors Affecting Anaerobic Digestion Process. In *Waste Bioremediation*; Varjani, S.J., Gnansounou, E., Gurunathan, B., Pant, D., Zakaria, Z.A., Eds.; Springer: Singapore, 2018; pp 343–359.
5. Clemens, H.; Bailis, R.; Nyambane, A.; Ndung'u, V. Africa Biogas Partnership Program: A review of clean cooking implementation through market development in East Africa. *Energy Sustain. Dev.* **2018**, *46*, 23–31. https://doi.org/10.1016/j.esd.2018.05.012.
6. Wang, W.; Lee, D.-J. Valorization of anaerobic digestion digestate: A prospect review. *Bioresour. Technol.* **2021**, *323*, 124626. https://doi.org/10.1016/j.biortech.2020.124626.
7. Kainthola, J.; Kalamdhad, A.S.; Goud, V.V. A review on enhanced biogas production from anaerobic digestion of lignocellulosic biomass by different enhancement techniques. *Process Biochem.* **2019**, *84*, 81–90. https://doi.org/10.1016/j.procbio.2019.05.023.
8. Li, Y.; Park, S.Y.; Zhu, J. Solid-state anaerobic digestion for methane production from organic waste. *Renew. Sustain. Energy Rev.* **2011**, *15*, 821–826. https://doi.org/10.1016/j.rser.2010.07.042.
9. Bensah, E.C.; Mensah, M.; Antwi, E. Status and prospects for household biogas plants in Ghana—Lessons, barriers, potential, and way forward. *Int. J. Energy Environ.* **2011**, *2*, 887–898.
10. Ganesh, R.; Torrijos, M.; Sousbie, P.; Lugardon, A.; Steyer, J.P.; Delgenes, J.P. Single-phase and two-phase anaerobic digestion of fruit and vegetable waste: Comparison of start-up, reactor stability and process performance. *Waste Manag.* **2014**, *34*, 875–885. https://doi.org/10.1016/j.wasman.2014.02.023.
11. Agrawal, A.; Chaudhari, P.K.; Ghosh, P. Anaerobic digestion of fruit and vegetable waste: A critical review of associated challenges. *Environ. Sci. Pollut. Res.* **2022**, *30*, 24987–25012. https://doi.org/10.1007/s11356-022-21643-7.
12. Zia, M.; Ahmed, S.; Kumar, A. Anaerobic digestion (AD) of fruit and vegetable market waste (FVMW): Potential of FVMW, bioreactor performance, co-substrates, and pre-treatment techniques. *Biomass. Conv. Bioref.* **2022**, *12*, 3573–3592. https://doi.org/10.1007/s13399-020-00979-5.
13. Filer, J.; Ding, H.H.; Chang, S. Biochemical Methane Potential (BMP) Assay Method for Anaerobic Digestion Research. *Water* **2019**, *11*, 921. https://doi.org/10.3390/w11050921.
14. Yoon, Y.; Lee, S.; Kim, K.; Jeon, T.; Shin, S. Study of anaerobic co-digestion on wastewater treatment sludge and food waste leachate using BMP test. *J Mater Cycles Waste Manag* **2018**, *20*, 283–292. https://doi.org/10.1007/s10163-017-0581-9.
15. Demirer, G.N.; Duran, M.; Güven, E.; Ugurlu, Ö.; Tezel, U.; Ergüder, T.H. Anaerobic treatability and biogas production potential studies of different agro-industrial wastewaters in Turkey. *Biodegradation* **2000**, *11*, 401–405. https://doi.org/10.1023/a:1011659705369.

16. Suhartini, S.; Pangestuti, M.B.; Dewanti, B.S.; Hidayat, N. Textile wastewater treatment: Biodegradability on aerobic and anaerobic process. *IOP Conf. Ser. Earth Env. Sci.* **2019**, *230*, 012091. https://doi.org/10.1088/1755-1315/230/1/012091.
17. Caillet, H.; Lebon, E.; Akinlabi, E.; Madyira, D.; Adelard, L. Influence of inoculum to substrate ratio on methane production in Biochemical Methane Potential (BMP) tests of sugarcane distillery waste water. *Procedia Manuf.* **2019**, *35*, 259–264. https://doi.org/10.1016/j.promfg.2019.05.037.
18. Baek, G.; Kim, D.; Kim, J.; Kim, H.; Lee, C. Treatment of Cattle Manure by Anaerobic Co-Digestion with Food Waste and Pig Manure: Methane Yield and Synergistic Effect. *Int. J. Environ. Res. Public Health* **2020**, *17*, 4737. https://doi.org/10.3390/ijerph17134737.
19. Hilgert, J.E.; Herrmann, C.; Petersen, S.O.; Dragoni, F.; Amon, T.; Belik, V.; Ammon, C.; Amon, B. Assessment of the biochemical methane potential of in-house and outdoor stored pig and dairy cow manure by evaluating chemical composition and storage conditions. *Waste Manag.* **2023**, *168*, 14–24. https://doi.org/10.1016/j.wasman.2023.05.031.
20. Nasir, I.M.; Mohd Ghazi, T.I.; Omar, R. Anaerobic digestion technology in livestock manure treatment for biogas production: A review. *Eng. Life Sci.* **2012**, *12*, 258–269. https://doi.org/10.1002/elsc.201100150.
21. Nieto, P.P.; Hidalgo, D.; Irusta, R.; Kraut, D. Biochemical methane potential (BMP) of agro-food wastes from the Cider Region (Spain). *Water Sci. Technol.* **2012**, *66*, 1842–1848. https://doi.org/10.2166/wst.2012.372.
22. Elbeshbishy, E.; Nakhla, G.; Hafez, H. Biochemical methane potential (BMP) of food waste and primary sludge: Influence of inoculum pre-incubation and inoculum source. *Bioresour. Technol.* **2012**, *110*, 18–25. https://doi.org/10.1016/j.biortech.2012.01.025.
23. Addae, G.; Oduro-Kwarteng, S.; Fei-Baffoe, B.; Rockson, M.A.D.; Ribeiro, J.X.F.; Antwi, E. Market waste composition analysis and resource recovery potential in Kumasi, Ghana. *J. Air Waste Manag. Assoc.* **2021**, *71*, 1529–1544. https://doi.org/10.1080/10962247.2021.1969296.
24. Azasi, V.D.; Offei, F.; Kemausuor, F.; Akpalu, L. Bioenergy from crop residues: A regional analysis for heat and electricity applications in Ghana. *Biomass Bioenergy* **2020**, *140*, 105640. https://doi.org/10.1016/j.biombioe.2020.105640.
25. Arthur, R.; Glover, K. Biomethane potential of the POME generated in the palm oil industry in Ghana from 2002 to 2009. *Bioresour. Technol.* **2012**, *111*, 155–160. https://doi.org/10.1016/j.biortech.2012.02.065.
26. Yu, Z.; Leng, X.; Zhao, S.; Ji, J.; Zhou, T.; Khan, A.; Kakde, A.; Liu, P.; Li, X. A review on the applications of microbial electrolysis cells in anaerobic digestion. *Bioresour. Technol.* **2018**, *255*, 340–348. https://doi.org/10.1016/j.biortech.2018.02.003.
27. Pandit, S.; Savla, N.; Sonawane, J.M.; Sani, A.M.; Gupta, P.K.; Mathuriya, A.S.; Rai, A.K.; Jadhav, D.A.; Jung, S.P.; Prasad, R. Agricultural Waste and Wastewater as Feedstock for Bioelectricity Generation Using Microbial Fuel Cells: Recent Advances. *Fermentation* **2021**, *7*, 169. https://doi.org/10.3390/fermentation7030169.
28. Palmonari, A.; Cavallini, D.; Sniffen, C.; Fernandes, L.; Holder, P.; Fagioli, L.; Fusaro, I.; Biagi, G.; Formigoni, A.; Mammi, L. Short communication: Characterization of molasses chemical composition. *J. Dairy Sci.* **2020**, *103*, 6244–6249. https://doi.org/10.3168/jds.2019-17644.
29. Wang, B.; Nges, I.A.; Nistor, M.; Liu, J. Determination of methane yield of cellulose using different experimental setups. *Water Sci. Technol.* **2014**, *70*, 599–604. https://doi.org/10.2166/wst.2014.275.
30. HHolliger, C.; Alves, M.; Andrade, D.; Angelidaki, I.; Astals, S.; Baier, U.; Bougrier, C.; Buffière, P.; Carballa, M.; de Wilde, V.; et al. Towards a standardization of biomethane potential tests. *Water Sci. Technol.* **2016**, *74*, 2515–2522. https://doi.org/10.2166/wst.2016.336.
31. Hansen, T.L.; Schmidt, J.E.; Angelidaki, I.; Marca, E.; Jansen, J.l.C.; Mosbæk, H.; Christensen, T.H. Method for determination of methane potentials of solid organic waste. *Waste Manag.* **2004**, *24*, 393–400. https://doi.org/10.1016/j.wasman.2003.09.009.
32. Angelidaki, I.; Alves, M.; Bolzonella, D.; Borzacconi, L.; Campos, J.L.; Guwy, A.J.; Kalyuzhnyi, S.; Jenicek, P.; van Lier, J.B. Defining the biomethane potential (BMP) of solid organic wastes and energy crops: A proposed protocol for batch assays. *Water Sci. Technol.* **2009**, *59*, 927–934. https://doi.org/10.2166/wst.2009.040.
33. Hafner, S.D.; Fruteau, De Laclos, H.; Koch, K.; Holliger, C. Improving Inter-Laboratory Reproducibility in Measurement of Biochemical Methane Potential (BMP). *Water* **2020**, *12*, 1752. https://doi.org/10.3390/w12061752.
34. Kafle, G.K.; Chen, L. Comparison on batch anaerobic digestion of five different livestock manures and prediction of biochemical methane potential (BMP) using different statistical models. *Waste Manag.* **2016**, *48*, 492–493. https://doi.org/10.1016/j.wasman.2015.10.021.
35. Esparza-Soto, M.; Alcaraz-Ibarra, S.; Lucero-Chávez, M.; Jiménez-Moleón, M.d.C.; Mier-Quiroga, M.d.L.A.; Fall, C. First derivative of Gompertz equation: Identification of substrate fractions in psychrophilic anaerobic digestion. *Biocatal. Agric. Biotechnol.* **2025**, *66*, 103595. https://doi.org/10.1016/j.bcab.2025.103595.

36. Photiou, P.; Vyrides, I. Calcined eggshells in anaerobic digestion: Buffering acidification in AD and evaluating end products from phosphate adsorption as soil conditioners. *J. Environ. Chem. Eng.* **2022**, *10*, 107957. https://doi.org/10.1016/j.jece.2022.107957.
37. Chen, S.; Zhang, J.; Wang, X. Effects of alkalinity sources on the stability of anaerobic digestion from food waste. *Waste Manag. Res.* **2015**, *33*, 1033–1040. https://doi.org/10.1177/0734242x15602965.
38. Zbair, M.; Limousy, L.; Drané, M.; Richard, C.; Juge, M.; Aemig, Q.; Trably, E.; Escudié, R.; Peyrelasse, C.; Bennici, S. Integration of Digestate-Derived Biochar into the Anaerobic Digestion Process through Circular Economic and Environmental Approaches—A Review. *Materials* **2014**, *17*, 3527. https://doi.org/10.3390/ma17143527.
39. Devi, P.; Eskicioglu, C. Effects of biochar on anaerobic digestion: A review. *Environ. Chem. Lett.* **2024**, *22*, 2845–2886. https://doi.org/10.1007/s10311-024-01766-8.
40. Colantoni, S.; Molognoni, D.; Sánchez-Cueto, P.; De Soto, C.; Bosch-Jimenez, P.; Ghemis, R.; Borràs, E. Bioelectrochemically-improved anaerobic digestion of fishery processing industrial wastewater. *J. Water Process Eng.* **2024**, *65*, 105848. https://doi.org/10.1016/j.jwpe.2024.105848.
41. Molognoni, D.; Garcia, M.; Sánchez-Cueto, P.; Bosch-Jimenez, P.; Borràs, E.; Lladó, S.; Ghemis, R.; Karakachian, G.; Aemig, Q.; Bouteau, G. Electrochemical optimization of bioelectrochemically improved anaerobic digestion for agricultural digestates' valorisation to biomethane. *J. Environ. Manag.* **2025**, *373*, 123898. https://doi.org/10.1016/j.jenvman.2024.123898.
42. De Vrieze, J.; Raport, L.; Willems, B.; Verbrugge, S.; Volcke, E.; Meers, E.; Angenent, L.T.; Boon, N. IInoculum selection influences the biochemical methane potential of agro-industrial substrates. *Microb. Biotechnol.* **2015**, *8*, 776–786. https://doi.org/10.1111/1751-7915.12268.
43. Moraes, B.; Triolo, J.; Lecona, V.; Zaiat, M.; Sommer, S. Biogas production within the bioethanol production chain: Use of co-substrates for anaerobic digestion of sugar beet vinasse. *Bioresour. Technol.* **2015**, *190*, 227–234. https://doi.org/10.1016/j.biortech.2015.04.089.
44. Yang, G.; Zhang, P.; Zhang, G.; Wang, Y.; Yang, A. Degradation properties of protein and carbohydrate during sludge anaerobic digestion. *Bioresour. Technol.* **2017**, *73*, 892–903. https://doi.org/10.1016/j.biortech.2015.05.076.
45. Feng, L.; Li, Y.; Chen, C.; Liu, X.; Xiao, X.; Ma, X.; Zhang, R.; He, Y.; Liu, G. Biochemical Methane Potential (BMP) of Vinegar Residue and the Influence of Feed to Inoculum Ratios on Biogas Production. *BioResources* **2013**, *8*, 2487–2498. https://doi.org/10.15376/biores.8.2.2487-2498.
46. Teclu, D.; Tivchev, G.; Laing, M.; Wallis, M. Determination of the elemental composition of molasses and its suitability as carbon source for growth of sulphate-reducing bacteria. *J. Hazard. Mater.* **2009**, *161*, 1157–1165. https://doi.org/10.1016/j.jhazmat.2008.04.120.
47. Kryvoruchko, V.; Machmüller, A.; Bodiroza, V.; Amon, B.; Amon, T. Anaerobic digestion of by-products of sugar beet and starch potato processing. *Biomass Bioenergy* **2009**, *33*, 620–627. https://doi.org/10.1016/j.biombioe.2008.10.003.
48. Ji, C.; Kong, C.-X.; Mei, Z.-L.; Li, J. A Review of the Anaerobic Digestion of Fruit and Vegetable Waste. *Appl. Biochem. Biotechnol.* **2017**, *183*, 906–922. https://doi.org/10.1007/s12010-017-2472-x.
49. Chen, Y.; Cheng, J.J.; Creamer, K.S. Inhibition of anaerobic digestion process: A review. *Bioresour. Technol.* **2008**, *99*, 4044–4064. https://doi.org/10.1016/j.biortech.2007.01.057.
50. Rajagopal, R.; Massé, D.I.; Singh, G. A critical review on inhibition of anaerobic digestion process by excess ammonia. *Bioresour. Technol.* **2013**, *143*, 632–641. https://doi.org/10.1016/j.biortech.2013.06.030.
51. Zhao, J.; Liu, Y.; Wang, D.; Chen, F.; Li, X.; Zeng, G.; Yang, Q. Potential impact of salinity on methane production from food waste anaerobic digestion. *Waste Manag.* **2017**, *67*, 308–314. https://doi.org/10.1016/j.wasman.2017.05.016.
52. Edwiges, T.; Frare, L.; Mayer, B.; Lins, L.; Triolo, J.M.; Flotats, X.; De Mendonça Costa, M.S.S. Influence of chemical composition on biochemical methane potential of fruit and vegetable waste. *Waste Manag.* **2018**, *71*, 618–625. https://doi.org/10.1016/j.wasman.2017.05.030.
53. Suhartini, S.; Nurika, I.; Paul, R.; Melville, L. Estimation of Biogas Production and the Emission Savings from Anaerobic Digestion of Fruit-based Agro-industrial Waste and Agricultural crops residues. *Bioenerg. Res.* **2021**, *14*, 844–859. https://doi.org/10.1007/s12155-020-10209-5.
54. Zhai, N.; Zhang, T.; Yin, D.; Yang, G.; Wang, X.; Ren, G.; Feng, Y. Effect of initial pH on anaerobic co-digestion of kitchen waste and cow manure. *Waste Manag.* **2015**, *38*, 126–131. https://doi.org/10.1016/j.wasman.2014.12.027.
55. Appels, L.; Baeyens, J.; Degrève, J.; Dewil, R. Principles and potential of the anaerobic digestion of waste-activated sludge. *Prog. Energy Combust. Sci.* **2008**, *34*, 755–781. https://doi.org/10.1016/j.pecs.2008.06.002.

56. Chuenchart, W.; Logan, M.; Leelayouthayotin, C.; Visvanathan, C. Enhancement of food waste thermophilic anaerobic digestion through synergistic effect with chicken manure. *Biomass Bioenergy* **2020**, *136*, 105541. https://doi.org/10.1016/j.biombioe.2020.105541.
57. Torres, C.I.; Krajmalnik-Brown, R.; Parameswaran, P.; Marcus, A.K.; Wanger, G.; Gorby, Y.A.; Rittmann, B.E. Selecting Anode-Respiring Bacteria Based on Anode Potential: Phylogenetic, Electrochemical, and Microscopic Characterization. *Environ. Sci. Technol.* **2009**, *43*, 9519–9524. https://doi.org/10.1021/es902165y.
58. Zhen, G.; Kobayashi, T.; Lu, X.; Xu, K. Understanding methane bioelectrosynthesis from carbon dioxide in a two-chamber microbial electrolysis cells (MECs) containing a carbon biocathode. *Bioresour. Technol.* **2015**, *186*, 141–148. https://doi.org/10.1016/j.biortech.2015.03.064.
59. Arthur, R.; Baidoo, M.F.; Antwi, E. Biogas as a potential renewable energy source: A Ghanaian case study. *Renew. Energy* **2011**, *36*, 1510–1516. https://doi.org/10.1016/j.renene.2010.11.012.
60. Rao, P.V.; Baral, S.S.; Dey, R.; Mutnuri, S. Biogas generation potential by anaerobic digestion for sustainable energy development in India. *Renew. Sustain. Energy Rev.* **2010**, *14*, 2086–2094. https://doi.org/10.1016/j.rser.2010.03.031.
61. Wang, B.; Strömberg, S.; Li, C.; Nges, I.A.; Nistor, M.; Deng, L.; Liu, J. Effects of substrate concentration on methane potential and degradation kinetics in batch anaerobic digestion. *Bioresour. Technol.* **2015**, *194*, 240–246. https://doi.org/10.1016/j.biortech.2015.07.034.
62. Kadam, R.; Panwar, N.L. Recent advancement in biogas enrichment and its applications. *Renew. Sustain. Energy Rev.* **2017**, *73*, 892–903. https://doi.org/10.1016/j.rser.2017.01.167.